國 立 交 通 大 學

環 境 工 程 研 究 所

碩 士 論 文

地下水污染源歷程重建：模擬退火演算法

Reconstructing the Release History of a Groundwater Contaminant Using Simulated Annealing

研 究 生：陳 淇 汾

指導教授：葉 弘 德 教授

中 華 民 國 九 十 五 年 七 月

地下水污染源歷程重建：模擬退火演算法

Reconstructing the release history of a groundwater contaminant using simulated annealing

研 究 生 ： 陳淇汾　　Student：Chi-Fen Chen

指導教授： 葉弘德　　Advisor：Hund-Der Yeh

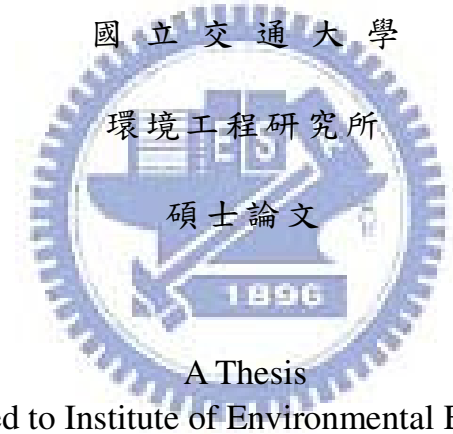

國 立 交 通 大 學

環境工程研究所

碩士論文

A Thesis
Submitted to Institute of Environmental Engineering
College of Engineering
National Chiao Tung University
in Partial Fulfillment of the Requirements
for the Degree of
Master of Science
in
Environmental Engineering
June, 2006
Hsinchu, Taiwan

中 華 民 國 九 十 五 年 七 月

地下水污染源歷程重建：模擬退火演算法

研究生：陳淇汾　　指導教授：葉弘德

國立交通大學環境工程研究所

摘要

當一個場址發現地下水有污染，且其已知污染源位置上曾更替過數個工廠或工廠的經營者時，重建污染源釋放歷程將可協助釐清各可能責任團體之責任歸屬問題。本研究利用函數擬合技巧，結合模擬退火演算法(simulated annealing, SA)與地下水污染傳輸控制方程式之基本解，來推算地下水污染源釋放歷程。其重建步驟為:首先，將已知釋放地點之真實污染源釋放函數代入地下水污染傳輸控制方程式之基本解中，計算得到監測井的污染物濃度值，然後設定此值為採樣濃度。其次視該污染源的釋放函數為未知，並假設其由多項指數函數所組成；利用 SA 試誤產生未知函數中的參數值，得到試誤之污染源釋放函數。隨後，將試誤函數代入地下水污染傳輸控制方程式之基本解中，計算出監測井的模擬濃度值。根據模擬濃度與採樣濃度之最小誤差平方和，SA 最後能搜尋到假設函數中之最佳參數值；若將此函數算出或畫出圖形曲線，則得以重建地下水污染源的釋放歷程。

為了模擬現地可能之情形，本研究分析的案例，從一維點源傳輸

問題擴展至二維與三維非點源傳輸案例；另外考慮含水層為有限寬度與無限寬度兩種不同狀況。本研究除了調查監測井與污染源的距離對重建結果的影響，同時也針對幾項問題進行探討，分別是時間性數據與空間性數據在污染源釋放歷程重建上之應用、兩個獨立污染源釋放歷程之鑑定、地下水污染傳輸之延散效應與生物降解反應、及採樣濃度量測誤差與採樣濃度數據數目多寡對歷程重建結果之影響等。最後，整合所有結果的分析，提出一個重建污染源歷程的準則。

Reconstructing the release history of a groundwater contaminant using simulated annealing

Student: Chi-Fen Chen **Advisor: Hund-Der Yeh**

Institute of Environmental Engineering
Nation Chiao Tung University

ABSTRACT

As a site is found to have groundwater contamination, the reconstruction of the source release history can provide helpful forensic information to identify the responsible parties at a known source location since the owner of the contaminated source changes several times. The objective of this study is to use a function-fitting technique and simulated annealing (SA) incorporated with a fundamental solution of the groundwater transport equation to recover the source release history of a groundwater contamination. The source release history is recovered via a two-step process. In the first step, the fundamental solution for a "true" contaminant release function at a known source location is used to create the sampling concentrations at monitoring wells. In the second step, the "true" source release function, an unknown to be recovered, is assumed as a combination of several exponential functions; the SA generates trial values for the parameters in the assumed release function. The simulated concentrations are then obtained from the fundamental solution with the trial source release function. While minimizing the sum of square errors between the

simulated and sampling concentrations, SA can determine the optimal parameters of the assumed release function. The curve of source release history can be drawn based on the obtained parameters of the release function.

In order to have better representation to the field conditions, the problems of two- and three-dimensional plume originated from a non-point source are taken into account. In addition, two different aquifer configurations are considered; one has infinite width while the other has finite width. Besides, topics of measurement errors, contaminant biodegradation, the degree of dispersion, the location of monitoring well, the number of sampling data, the use of temporal concentration data or spatial concentration data, and the existence of two contaminated sources are also studied. Finally, a guideline for the optimal sampling strategy to reconstruct the source release history is recommended.

致謝

哈!哈!我的論文終於完成了，這必須要感謝許多人。首先我要感謝我的指導教授葉弘德老師，謝謝他對我嚴謹的指導與教誨，以及不吝於分享關於蝴蝶與花草的經驗與知識，讓我除了學會如何去解決問題外，也增加了自己對週遭事物的關心。其次，要感謝口試委員葉高次教授、童慶斌教授、陳主惠教授、劉振宇教授對本論文的指正與建議，使本論文得以更為完整。

當然，我還要感謝 GW 大家族：謝謝"成熟穩重"的智澤、郁仲、彥禎、雅琪、彥如、嘉真等學長姐的關心與鼓勵，快要退伍的桐樺學長，即將入伍的易璁同學，以及"活潑搞笑"的敏筠、毓婷、凱茹、士賓、博傑等學弟妹的協助與陪伴。

感謝環工所各研究群的伙伴們，你們讓我娛樂不匱乏；感謝思敏帶我認識新環境；感謝聯合的同學文杰、壯宇、偉鴻、騰毅、泩棱、寶仁你們在遠方的支持。感謝我的好朋友們；謝謝婉彣聽我抱怨，幫我排解苦悶；謝謝嘉惠與俊賢給我祝福；還有謝謝蔡定裕。

最後，我最最需要感謝的就是我的父母、姐姐、姐夫、詩晴跟長廷，謝謝你們的包容、關心和愛，讓我可以順利地完成我的學業，繼續人生的另一個階段。真的很感謝大家的幫忙，謝謝！

淇汾　謹致於

交通大學環境工程研究所

2006年7月

TABLE OF CONTENTS

LIST OF TABLES

LIST OF FIGURES

NOTATION

a_i	A coefficient defined by Eq.(18)
a_j	The release strength of the plume
B	Width of the aquifer [L]
B_1	Beginning coordinate of the source in the y-direction
B_2	Ending coordinate of the source in the y-direction
C	Concentration
$\partial C/\partial t$	The change in solute concentration with time [$ML^{-3}T^{-1}$]
$C(x, y, z, t)$	The contaminant concentration in the groundwater [ML^{-3}]
$C_{ext}(x_n,T)$	The exact concentration at location x_n at time T
$C_{meas}(x_n,T)$	The measured concentration at location x_n at time T
C_{in}	Contaminant source release function [ML^{-3}]
C_{ini}	The ith contaminant source release function
$C^T_{i,est}$	The concentration estimated at ith measurement point at time T
$C^T_{i,obs}$	The concentration measured at ith measurement point at time T
D	The hydraulic dispersion coefficient tensor [L^2T^{-1}]
D_x	x-component of the dispersion tensor
D_y	y-component of the dispersion tensor
D_z	z-component of the dispersion tensor
E	The system energy
F	A kernel function defined by Eq.(7)
H	Depth of the aquifer [L]
H_1	Beginning coordinate of the source in the z-direction
H_2	Ending coordinate of the source in the z-direction
k	The number of the terms needed in exponential function
k_B	Boltzmann constant of nature which relates temperature to energy
K_d	Chemical degradation rate [T^{-1}]
K_e^*	Modified heat exchange coefficient
L_1	Beginning coordinate of the source in the x-direction
L_2	Ending coordinate of the source in the x-direction
$MAXEVL$	Maximum number of iteration to terminate the algorithm
$min\, f$	The objective function defined by Eq.(23)
n	The number of measurement points

NS	The number of cycles
NT	The number of iterations before temperature reduction
OFV	Objective function value
$P(E)$	Probability defined by Eq.(19) and (20)
R_d	Retardation factor
RT	A cooling temperature factor
t	Time
t_{evol}	The plume evolution times
t_j	The release times of the plume
T	Sampling time
T_{emp}	Temperature
$T_{initial}$	Initial temperature
v	Average linear velocity vector [LT^{-1}]
x	Longitudinal coordinate
x_i	The x coordinates of the ith plume source
x_n	The location of the nth sample
x_s	x-coordinate of a point source
X_i	Either function X_1 or X_2
X_1	A function defined by Eq.(8)
X_2	A function defined by Eq.(9)
y	Transfer coordinate
y_i	The y coordinates of the ith plume source
y_s	y-coordinate of a point source
Y_j	Either function Y_1, Y_2, Y_3, or Y_4
Y_1	A function defined by Eq.(10)
Y_2	A function defined by Eq.(11)
Y_3	A function defined by Eq.(12)
Y_4	A function defined by Eq.(13)
z	Vertical coordinate
z_s	z-coordinate of a point source
Z_k	Either function Z_1 or Z_2
Z_1	A function defined by Eq.(14)
Z_2	A function defined by Eq.(15)
δ_n	The random number from a Gaussian standard population
ε	The error magnitude

∇	Gradient operator
λ	Radioactive decay constant
τ	Time
k_i	i-th eigenvalue defined by Eq.(17)
ψ_i	i-th eigenfunction defined by Eq.(16)
σ	One standard deviation of the contaminant distribution
σ_j	The release width parameters of plume
σ^2	The variance of the distribution

CHAPTER 1 INTRODUCTION

1.1. Background

Recently, many soil and groundwater contamination events have been reported in Taiwan. These reports reveal that people's health may be impaired if living near the contaminated sites. Therefore, an effort should be made to investigate the contaminant source and assess the remedial measures. Generally speaking, groundwater contaminants may originate from the disposal of wastewater for various purposes. All sources and causes of contamination can be classified into two categories: point sources and non-point sources. Point sources, characterized by the presence of identifiable sources, include storage tanks, pipeline releases, and chemical manufacturing locations. Non-point sources are referred to as larger-scale and more diffuse contamination originated from many smaller sources; for example, the agricultural fertilizers leaching through soil and finally affecting aquifers (Todd and Mays, 2005).

Taiwan EPA promulgated the Soil and Groundwater Remediation Act in 2000 to require the remediation for groundwater contamination if the concentration exceeds regulation standard. However, the remediation of groundwater contamination may be expensive, and the responsible party rather than the public should pay the costs. In addition, the assessment of the remediation needs to know the total contaminant

mass before groundwater remediation. This information could be estimated while the source release history, including the release concentration and release time, is reconstructed. Therefore, recovering source release history can provide forensic information to determine the liability among the responsible parties.

1.2. Literature Review

Recovering the source release history of a plume is an ill-posed problem since contaminant transport in groundwater is a dispersive and irreversible process. In the past two decades, many researchers have investigated this problem. Atmadja and Bagtzoglou (2001) reviewed the methods that had been developed during the past 15 years to identify the contaminant source location and recover the time-release history. They classified the contaminant transport inversion methods into four categories. They are: (1) optimization approaches, (2) probabilistic and geo-statistical simulation approaches, (3) analytical solution and regression approaches, and (4) direct approaches.

Optimization approaches, the early methods to identify the pollution source by solving the advection-dispersion equation (ADE), are to run forward simulations first and check the solutions with the spatial observed data. Wanger (1992) combined groundwater flow and contaminant transport simulation with non-linear maximum likelihood estimation to determine optimal estimates of the unknown model

parameters and source characteristics based on observations of hydraulic head and contaminant concentration. He pointed out that the source could be characterized by a set of unknown parameters.

Probabilistic and geo-statistical simulation approaches are to identify the source release history of a plume relying on probabilistic framework. In these approaches, the recovered release history is considered as a random process, defined through its probability density function and its statistical moments, so it can be determined with uncertainty. Butera and Tanda (2003) adopted the geo-statistical approach to model the ADE backward in time. Their applications focus on the incorporation of an area and two point sources in two-dimensional groundwater flow system with infinite domain. Boano et al. (2005) also applied the geo-statistical method to identify the contaminant sources in river pollution problems. Similar to Butera and Tanda (2003), they considered an area source and two point sources. Woodbury et al. (1998) used the minimum relative entropy inversion (MRE) to reconstruct a three-dimension plume source. They explained how MRE inversion can be used as a measure of resolution in linear inversion, and indicated the temporal concentration data at a few wells can be used to reconstruct the release history of a groundwater contaminant.

Much effort has been directed to the theoretical and mathematical problems of the inverse estimation. Butcher and Gauthier (1994) used inverse analytical

techniques to estimate the residual DNAPL mass. They used a tractable analytical approximation to the problem and developed additional simplifications to yield a form that can be solved for the parameters of interest. Alapati and Kabala (2000) applied the nonlinear least-squares (NLS) method to recover the gradual and the catastrophic release scenarios from its spatial concentration data. They found that the NLS method could resolve the catastrophic release histories well, even in the presence of moderate measurement errors.

Direct approaches use deterministic methods to solve the governing equations reversely. Skaggs and Kabala (1994) used Tikhonov regularization (TR) to recover the release history of a plume. TR was used to obtain a best possible solution of a one-dimensional solute transport through a homogeneous medium with a complex contaminant release history. Skaggs and Kabala (1995) used the quasi-reversibility (QR) method for the same problem solved in TR method. In QR method, a moving coordinate system was used to account for the velocity term of the ADE. Skaggs and Kabala (1998) extended their study of TR and employed Monte Carlo approach to infer the ability of recovering an arbitrary plume in a transport medium with dispersive characteristics.

Although previous literatures provide various methods to solve the source release history recovery problem, most of them only considered one kind of source

geometries, e. g., point source or area source; in addition, they all utilize more than 36 sampling concentrations to recover the source release history of a groundwater contaminant.

1.3. Objectives

The objective of this thesis is to design a novel method capable of solving the source release history recovery problem in an easy and effective way and to demonstrate that the proposed method is applicable to point source and non-point source cases as well. The method combines a function-fitting technique and simulated annealing (SA) with a fundamental solution of ADE. The solution of ADE describes the contaminant released from a source into a homogeneous aquifer. Therefore, the sampling concentrations in the stage of model development can be created from the fundamental solution at a known location with a "true" release function. For source release history recovery problem, the release history at a specific source location is unknown and can be estimated by a function-fitting technique. The source release history is assumed as a combination of several exponential functions, and SA based on trial and error assessment generates the values of parameters in the assumed release function. The simulated concentrations are then calculated by the fundamental solution with the trial source release function. While minimizing the sum of square errors between the simulated and sampling

concentrations, SA can determine the optimal parameters of the assumed release function. Finally, the curve of source release history could be easily observed after plotting the determined function.

Various field cases of the contaminant transport in one-, two-, and three-dimensions are considered and analyzed by the proposed approach. In addition, three types of contaminant source geometries and two different aquifer configurations are evaluated. The source geometries include point, area, and volume sources. The aquifer configurations contain both infinite width and finite width aquifers. Besides, both spatial and temporal concentration data are used to analyze the influences of contaminant biodegradation, the location of monitoring well, the degree of dispersion, measurement errors, and the number of sampling data on the results of reconstruction. An aquifer system may be polluted by several different contaminant sources at known spots; therefore, whether the method could distinguish the contamination proportions between two adjacent sources is investigated, too. Finally, a general guideline regarding to the sampling period and sampling region in recovering the source release history is also provided.

CHAPTER 2 METHODS

2.1 Advection-Dispersion Equation

Advection and hydrodynamic dispersion are the main mechanisms that make the dissolved contaminant spread and migrate in groundwater. Advection, the most significant mass transport process that the contaminant carried by the flowing groundwater, results from the gradient in fluid head. Hydrodynamic dispersion, a microscopic phenomenon, is caused by a combination of mechanical dispersion and molecular diffusion. Mechanical dispersion causes contaminant to spread out, owing to the variation of flow path and velocity in the groundwater movement. Molecular diffusion is the process in which the contaminants move from high concentration area to low concentration area due to concentration gradient.

For a steady uniform flow, the ADE for contaminant transport in saturated, homogeneous and isotropic porous media may be written as (Yeh, 1981):

$$\frac{\partial C}{\partial t} = \nabla(D \cdot \nabla C) - \nabla(vC) - \left(\frac{K_d}{R_d} + \lambda\right)C \qquad (1)$$

where $\partial C/\partial t$ is the change in solute concentration with time [$ML^{-3}T^{-1}$], ∇ is gradient operator, D is the hydraulic dispersion coefficient tensor [L^2T^{-1}], v is the average linear velocity in x- direction [LT^{-1}], K_d is the degradation rate [T^{-1}], λ is the radioactive decay constant [T^{-1}], and R_d is the retardation factor.

For source release history recovery problem, the source location is known. The source release history of a groundwater contaminant could be identified by solving Eq. (1) with reversed time subject to following initial and boundary conditions:

$$C(x, y, z, 0) = 0 \tag{2}$$

$$C(x_s, y_s, z_s, t) = C_{in}(t) \tag{3}$$

$$C(\pm\infty, y, z, t) = 0 \tag{4}$$

$$C(x, \pm\infty, z, t) = 0 \tag{5}$$

where x_s, y_s, and z_s are the x, y, and z coordinates of the plume source, respectively, and $C_{in}(t)$ is the contaminant source release function.

Contaminant transport is a dispersive and irreversible process; as a result, modeling groundwater contaminant transport with reversed time is an ill-posed problem whose solution does not satisfy general condition of uniqueness or stability. Accordingly, the strategy of the proposed method is to avoid solving the ill-posed problem directly. Instead, a relative well-posed problem is formulated and solved.

2.2 Analytical Modeling

The relative well-posed problem relies on a framework of an analytical model. Analytical model is one of useful and convenient tools for analyzing and predicting groundwater contaminant transport for a field contamination problem. Therefore, an analytical transient, one-, two-, and/or three-dimensional model (AT123D) developed

by Yeh (1981) is used to simulate the spatial-temporal concentration distribution of contaminant in a groundwater flow system. Assume that the aquifer is homogeneous and isotropic, the flow is steady and uniform, and the source release is continuous. The solution for Eq. (1) subject to initial and boundary conditions of Eqs. (2) - (5) can be written as:

$$C(x, y, z, t) = \int_0^T C_{in}(\tau) F(x, y, z, T-\tau) d\tau \tag{6}$$

where T is the sampling time, $C(x, y, z, T)$ is the plume concentration in the groundwater [ML^{-3}], and $F(x, y, z, T-\tau)$ is the fundamental solution of ADE, or called kernel function. Notice that the function $F(x, y, z, T-\tau)$ is chosen dependent on the source geometry and aquifer configuration. In AT123D, $F(x, y, z, T-\tau)$ for three-dimensional case is expressed as:

$$F(x, y, z, T-\tau) = X_i Y_j Z_k \tag{7}$$

where X, Y, and Z denote the source in x, y, and z direction, respectively, and the subscripts i, j, and k signify the type of source geometries and aquifer configurations.

The AT123D contains various options and these options are the combination of different type of contaminants, source geometries, source release, and aquifer configurations. In this study, three types of source geometries and two kinds of aquifer configurations are considered. The source geometries are point, area, and volume sources; the aquifer configurations are finite width and infinite width. Hence,

the functions X_i, Y_j, and Z_k, chosen from AT123D, are given as follows:

for point source in the *x*-direction:

$$X_1 = \frac{1}{\sqrt{4\pi D_x (T-\tau)}} \exp\left[-\frac{\{(x-x_s)-v(T-\tau)\}^2}{4D_x(T-\tau)} - \left(\frac{K_d}{R_d}+\lambda\right)(T-\tau) \right] \tag{8}$$

for line source in *x*-direction:

$$X_2 = \frac{1}{2}\left[erf\left(\frac{x-L_1-v(T-\tau)}{\sqrt{4D_x(T-\tau)}} \right) - erf\left(\frac{x-L_2-v(T-\tau)}{\sqrt{4D_x(T-\tau)}} \right) \right] \cdot \exp\left[-\left(\frac{K_d}{R_d}+\lambda\right)(T-\tau) \right] \tag{9}$$

for finite width and point source in the *y*-direction:

$$Y_1 = \frac{1}{B} + \frac{2}{B}\sum_{i=1}^{\infty} \cos\left(\frac{i\pi y}{B}\right) \cdot \cos\left(\frac{i\pi y_s}{B}\right) \cdot \exp\left[-\left(\frac{i\pi}{B}\right)^2 D_y (T-\tau) \right] \tag{10}$$

for finite width and line source in the *y*-direction:

$$Y_2 = \frac{B_2 - B_1}{B} + \frac{2}{B}\sum_{i=1}^{\infty} \cos\left(\frac{i\pi y}{B}\right) \cdot \frac{B}{i\pi} \left\{ \sin\left(\frac{i\pi B_2}{B}\right) - \sin\left(\frac{i\pi B_1}{B}\right) \right\} \exp\left[-\left(\frac{i\pi}{B}\right)^2 D_y (T-\tau) \right] \tag{11}$$

for infinite width and point source in the *y*-direction:

$$Y_3 = \frac{1}{\sqrt{4\pi D_y (T-\tau)}} \exp\left[-\frac{(y-y_s)^2}{4D_y(T-\tau)} \right] \tag{12}$$

for infinite width and line source in the *y*-direction:

$$Y_4 = \frac{1}{2}\left\{ erf\left(\frac{y-B_1}{\sqrt{4D_y(T-\tau)}} \right) - erf\left(\frac{y-B_2}{\sqrt{4D_y(T-\tau)}} \right) \right\} \tag{13}$$

for finite depth and point source in the *z*-direction:

$$Z_1 = \sum_{i=1}^{\infty} \psi_i(z)\psi_i(z_s) \cdot \exp\left[-k_i^{\,2} D_z (T-\tau) \right] + \frac{1}{H} \tag{14}$$

for finite depth and line source in the z-direction:

$$Z_2 = \frac{H_2 - H_1}{H} + \sum_{i=1}^{\infty} \psi_i(z) \left(\frac{a_i}{k_i} \right) \{ \sin(k_i H_2) - \sin(k_i H_1) - \frac{K_e^*}{D_z k_i} [\cos(k_i H_2) - \cos(k_i H_1)] \} \cdot \exp\left[- k_i^2 D_z (T - \tau) \right] \quad (15)$$

where B and H are respectively the width and the depth of the aquifer [L]; L_1, B_1, H_1 and L_2, B_2, H_2 are respectively the beginning and the end coordinates (x, y, z) of the source [L]; D_x, D_y and D_z are respectively the component of the dispersion tensor in x-, y-, and z- directions [L^2T^{-1}]; K_e^* is the modified heat exchange coefficient. In Eqs. (14) and (15), $\psi_i(z)$ is:

$$\psi_i(z) = a_i \left\{ \cos(k_i z) + \frac{K_e^*}{D_z k_i} \sin(k_i z) \right\} \quad (16)$$

where k_i and a_i are given as:

$$\tan(k_i H) = \frac{K_e^*}{D_z k_i} \quad (17)$$

and

$$a_i^2 = \frac{2}{H \left\{ 1 + \left(K_e^* / D_z k_i \right)^2 + \left(K_e^* / D_z X_i \right) \right\}} \quad (18)$$

The selection of fundamental function depends on the source geometry and aquifer condition. Once $F(x, y, z, T-\tau)$ is selected, the distribution of a groundwater plume concentration can be simulated by applying the Gaussian quadrature to estimate Eq. (6) with a given source release function, $C_{in}(\tau)$, and sampling time.

2.3 Optimization by SA

The following part will introduce how SA could determine the parameters of the assumed function in detail. SA is a heuristic search method, and the algorithm of SA is in analogy to thermodynamics of liquids freezing and crystallizing. If a hot liquid is cooled slowly, a pure crystal can be formed. This crystal is in the state of minimum energy for the system. However, if the liquid is cooled quickly, the pure crystal may not be formed, and the system may then be in the state of a local minimum energy. The energy probabilistic distribution of a system is expressed by Boltzmann probability distribution as:

$$P(E) \propto \exp\left(-E/\left(k_B T_{emp}\right)\right) \tag{19}$$

where the $P(E)$ is probability, E is the system energy, k_B is Boltzmann constant of nature which relates temperature to energy, and T_{emp} is the temperature. According to Eq. (19), the system has chance to run away from a local minimum energy to more global one, since lower probability may be occurred with high energy state at low temperature of a system (Press et al.,1986).

A modified Boltzmann probability function named as the Metropolis' criteria (Kirpatrick, 1983) is adopted in SA. The Metropolis' criteria supply a more efficient simulation of thermal motion of atoms in equilibrium of a given temperature. In each step of the simulation, an atom is given a random displacement and the

thermodynamics system is to change its configuration from energy E_1 to energy E_2. $\Delta E = E_2 - E_1$. If $\Delta E \leq 0$, the displacement is accepted, and the displaced atom is used as the starting point of the next step. The case $\Delta E > 0$ is treated probabilistically. The Metropolis' criteria are written as follows (Pham and Karaboga, 2000):

$$P(\Delta E) = \begin{cases} 1, & \text{if} \quad E_2 \leq E_1 \\ \exp\left[\dfrac{-(E_2 - E_1)}{k_B T_{emp}}\right], & \text{if} \quad E_2 > E_1 \end{cases} \tag{20}$$

If $E_2 > E_1$, one has to check the Metropolis' criteria. A random number uniformly distributed in interval (0, 1) is selected and compared with $P(\Delta E)$. If the random number is smaller than $P(\Delta E)$, then the displaced atom replaces the original one. Otherwise, the original atom is used to start the next step.

The procedure of SA is an iterative improvement, and the Metropolis' criteria provide a general inference of iterative improvement. To implement SA, an initial guess of the solution, called current optimal solution, is set to calculate the current objective function in analog of energy. Then, *NS* random trial solutions are created and the objective function values (OFV) of the trial solutions are computed by SA. Once the OFV of the trial solutions satisfies the Metropolis criteria, the trial solution is accepted and replaces the current optimal solution. Otherwise, the trial solution is rejected. After *NT* times through the loops, the temperature, *Te*, is reduced. As the temperature falls, SA slowly focuses on the most promising area. While SA acquires

the optimal solution or the system satisfies the terminal temperature or iteration numbers, the algorithm will be ceased.

CHAPTER 3 HISTORY RECOVERY PROCESS

In this chapter we illustrate the two-step process of the proposed method to recover the source release history of a groundwater contaminant. The first step is to create the sampling concentrations at the monitoring wells. A numerical example given in Skaggs and Kabala (1994) is employed to generate the sampling concentrations. The "true" source release function with a three sinuous waves for a non-reactive contaminant source given by Skaggs and Kabala (1994) was:

$$C_{in}(t) = \exp\left(-\frac{(t-130)^2}{2(5)^2}\right) + 0.3\exp\left(-\frac{(t-150)^2}{2(10)^2}\right) + 0.5\exp\left(-\frac{(t-190)^2}{2(7)^2}\right) \qquad (21)$$

where 130, 150, and 190 are the source release times; 5, 10, and 7 are a measure of the spread of the release function; 1, 0.3, and 0.5 are the release strength of source. The fundamental solution, $F(x, y, z, T-\tau)$, is chosen based on the source geometry and aquifer configuration. The distribution of plume concentration can be created based on Eqs. (6) and (21) with given aquifer parameters; thus, the sampling concentration data are acquired.

The second step is to apply the function-fitting technique to solve the source release history recovery problem. Lin (1999) mentioned that any continuous function on a closed and bounded interval can be approximated on that interval by exponential functions or polynomials. In other words, if a model can fit the

sampling data and produce a smooth curve, then it can be considered as a proper model. Accordingly, a source release function may be expressed as (Alapati and Kabala, 2000):

$$C_{in}(t) = \sum_{j=1}^{k} a_j \exp\left(\frac{-(t - t_j)^2}{2\sigma_j^2} \right) \tag{22}$$

where k is the number of the terms needed in exponential function, a_j is the release strength of the source, t_j is the release times of the source, and σ_j is the release width parameters of source. The value of k represents the number of source release waves; thus, $k = 3$ in Eq. (21).

The SA is applied to produce the trial values for parameters in Eq. (22), i.e., a_j, t_j, and σ_j. The simulated concentrations are then generated from Eqs. (6) and (22) with those trial parameters. The optimal parameter values can be determined as the objective function is minimized. The objective function in SA is expressed as

$$\min f = \sum_{i=1}^{n} \left(C_{i,sim}^{T} - C_{i,sam}^{T} \right)^2 \tag{23}$$

where $C^{T}_{i,sim}$ is the simulated concentration estimated at ith monitoring well at sampling time T, $C^{T}_{i,sam}$ is the sampling concentration measured at ith monitoring well at sampling time T, and n is the number of monitoring wells.

In SA, an initial guess of the parameters in the assumed function is set to calculate the simulated concentrations based on Eqs. (6) and (22), then the initial OFV is calculated by Eq. (23). The SA generates NS random trial solutions and computes

their OFV of the trial solutions. If the OFV of the trial solution is smaller than that of the current value, the trial solution is taken as the current optimal solution. If not, Metropolis' criteria are applied to accept or reject the poorer solution. The temperature is reduced after *NT* times through the above loops. The algorithm will be continued until SA obtains the optimal solution or the system satisfies the terminal temperature or iteration numbers.

The variable k in Eq. (22), representing the wave numbers in the source release function, is a crucial problem to solve. The value of k can be determined by selecting the one which has the least value of the OFV, or can be chosen directly based on the shape of the concentration distribution which to some extent reflects the pattern of the source release history

To employ SA, the number of trial solution for each unknown (*NS*) and the annealing schedule must be defined. The annealing schedule consists of the initial temperature ($T_{initial}$), a cooling temperature factor (*RT*), the iteration number before decreasing the temperature (*NT*), and maximum number of iteration to terminate the algorithm (*MAXEVL*). No general rule is applicable in choosing these parameters. In this study, $T_{initial}$, *NS*, *NT*, *RT*, and *MAXEVL* are given as 100, 30, 5, 0.8, and 10^6 respectively. Generally speaking, good values for those parameters can be obtained

by trial-and error approach. Poor guesses will give spikes in the recovered release history instead of smooth release function curve.

CHAPTER 4 SCENARIOS AND RESULTS

Nine scenarios are designed to demonstrate the proposed method in solving the source release history recovery problem. Scenarios 1 – 3 are intended to show that the proposed method is applied to the case of one-dimensional point source and then to the case of two- and three-dimensional non-point sources. In addition, two different aquifer configurations are considered for two- and three-dimensional groundwater transport; one is that the aquifer has infinite width while the other considers the width of the aquifer is finite. Scenario 1 attempts to recover a point source release history for contaminant in one-, two-, and three- dimensional transports. Scenario 2 aims to reconstruct an area source release history for contaminant in two-, and three-dimensional transports. Scenario 3 aspires to recover a volume source release history for contaminant in three-dimensional transport. The effect of contaminant biodegradation on the result of reconstruction is also investigated in scenario 3. These three scenarios employ spatial concentration data sampled from 17 monitoring wells.

Scenario 4 is used to investigate whether the temporal concentration data sampled at few wells could recover the source release history or not because more spatial concentration data implying higher cost involved in installing monitoring wells. The number of monitoring wells considered is from one to four. Scenario 5 is to

explore the required numbers of temporal concentration data for solving the source history recovery problem. In scenario 6, temporal concentration data are utilized to establish a general guideline on the sampling period and sampling region in recovering the source release history.

Scenario 7 intends to prove that the guideline drawn from scenario 6 is also applicable to analyze the spatial concentration data. In scenario 8, normally distributed noise is added to the sampling concentrations to investigate the capability of the proposed method in recovering the source release history. An aquifer system may be polluted by several sources at different times from known locations. Therefore, scenario 9 is to test whether the proposed method can handle the composite contamination form two adjacent sources or not. The influences of the location of monitoring wells and the degree of dispersion on the result of recovering release history are also explored in scenario 9.

Since this study is based on the analytical approach to recover the source history, each scenario assumes that the aquifer is homogeneous and isotropic; the flow is steady and uniform; the contaminant is conservative, no decay, and no adsorbed on the aquifer. Various aquifer parameters and the source geometry and location are assumed known.

4.1 Scenario 1: Point Source

Scenario 1 attempts to recover a point source release history for contaminant in one-, two-, and three- dimensional transports. Five cases are designed to assess the applicability of the proposed approach. Assume the point source is located at the origin, i.e., $(x_s, y_s, z_s) = (0, 0, 0)$, and the aquifer is clean and the background concentration is zero at the beginning. Suppose the aquifer is infinite in x-direction and finite in z-direction ($0 < z < 3$ m). Two types of aquifer configurations are considered; one has an infinite width while the other has a finite width in y-direction.

In case 1, a one-dimensional plume in the x-direction with the kernel function, F, equaling X_1 in Eq. (8) is considered. In case 2, a two-dimensional transport in the x-y plane with $F = X_1 Y_3$ in Eqs. (8) and (12) is studied. In case 3, a three-dimensional plume with $F = X_1 Y_3 Z_1$ in Eqs. (8), (12), and (14) is investigated. For cases 2 and 3, the aquifer is infinite in y-direction while for cases 4 and 5, the aquifer has a finite width of 100 m. Case 4 supposes the plume is two-dimensional and distributed in the x-y plane with $F = X_1 Y_1$ in Eqs. (8) and (10). Case 5 assumes to have a three-dimensional plume with $F = X_1 Y_1 Z_1$ in Eqs. (8), (10), and (14).

With Eqs. (6) and (21), the plume concentration is estimated by using the parameters v, D_x, D_y, and D_z being equal to 1 m/day, 1 m^2/day, 0.1 m^2/day, and 0.1 m^2/day, respectively. Figure 1 shows the plume concentration at 225 days for cases

1 – 5, revealing that the originally three distinct release waves of the source have been released at 225 days. The monitoring wells are installed from 0 m to 160 m with a uniform interval of 10m along x-axis. Thus, 17 spatial concentration data are available for recovering the source release history.

A function fitting technique is applied to solve the source release history recovery problem, and the source release history of groundwater contaminant is represented by Eq. (22) which contains three parameters, a_j, t_j, and σ_j. Totally $3k$ unknowns have to be determined with 17 sampling data. Therefore, the value of k can be up to five. Figure 1 shows the sampling concentration distributions with two waves for cases 1 – 5, indicating the number of k is two at least. Accordingly, it suggests trying the value of two to five to find the best k based on the OFV. The best possible k occurs when the OFV is the least.

Table 1(a) lists the OFV for different k in cases 1 – 5, indicating that the objective function has a least value when $k = 3$. Table 2 shows the estimated parameters determined by SA, also revealing that the estimated release history function is exact when $k = 3$. Hence, we conclude that the release history is recovered when the OFV is the least among different k. Figure 2 displays the recovered release histories of the five cases when $k = 3$. For case 1, the reconstruction shown in Fig. 2(a) is in good agreement with the true one. For

aquifer with infinite width, the release history represented by the dashed line shown in Figs. 2(b) and 2(c) for cases 2 and 3 respectively is recovered acceptably, except the first wave is somewhat underestimated. In contrast, the first pattern of the reconstruction gives a little overestimation in cases 4 and 5 for aquifer with a finite width of 100 m, as displayed in Figs. 2(b) and 2(c), respectively. Those results confirm that the proposed approach gives good estimated results as compared with the true one. In other words, the exponential function is suitable to use as the basis of the release history and the SA can successfully estimate the parameters (the release strength, release times, and release width) of the source release history as well.

However, attention should be paid to the OFV when k = 4 in cases 2, 3, and 5, since it is close to the OFV when k = 3. Figure 3 displays the recovered release history when k = 4 for cases 2, 3, and 5, with one spike appeared in the reconstructed history. In case 2, the spike occurs at 172 days while it appears at 88 and 163 days in cases 3 and 5, respectively. In addition, the first wave in case 3 and the middle wave in case 5 are overestimated. These results indicate that the source release history recovered for the case with OFV, which is not the least one, can lead to a poor reconstruction.

4.2 Scenario 2: Area Source

For the real field problem, the use of point source is a simplified assumption since the source geometry of contamination to some extent has dimension, e.g., source discharging from irrigation practices or fertilizer applications. Therefore, scenario 2 aims to reconstruct the release history of an area source for contaminant in two- and three-dimensional transports. Four cases are designed to analyze the application of the proposed method while considering two aquifer configurations of finite width and infinite width. The aquifer dimensions and the aquifer parameters are set the same as scenario 1. The dimensions of the area source are 5m × 5m.

The sampling concentrations can be calculated based on Eqs. (6) and (21) with appropriate kernel functions. In case 1, the two-dimensional transport in the *x*-*y* plane with $F = X_2 Y_4$ in Eqs. (9) and (13). In case 2, the proposed method is used to recover the release history of a three-dimensional plume with $F = X_2 Y_4 Z_1$ in Eqs. (9), (13), and (14). Consider the aquifer is infinite in the *y*-direction in cases 1 and 2 while it is finite with the width of 100 m in cases 3 and 4. Case 3 considers that the plume is two-dimensional and distributed in the *x*-*y* plane with $F = X_2 Y_2$ in Eqs. (9) and (11). Case 4 assumes to have a three-dimensional plume with $F = X_2 Y_2 Z_1$ in Eqs. (9), (11), and (14).

The spatial concentration data at 225 days for those four cases are shown in Fig.

4, displaying 17 sampling concentrations are available to reconstruct the source release history. Since $3k$ unknowns are to be determined with 17 sampling data and the sampling concentration distributions shown in Fig. 4 imply that the number of release waves of the source is at least two. Thus, the number of source release waves, k, is chosen from two to five to find the suitable k which occurs when the OFV has a least value. Table 1(b) lists the estimated OFV for different k in cases 1 – 4, indicating that the least OFV occurs when $k = 3$, except case 1 in which the least OFV occurs when $k = 4$.

Table 3 lists the estimated parameter values determined by SA for those four cases. The results indicate that the estimated source release function in each case is exact when $k = 3$. However, the estimated k is 4 for the recovered release history in case 1 since it has the least OFV. Figure 5 shows that an expected spike occurs at 184 days in the recovered history when $k = 4$ in case 1. Because a smooth curve for the release history is a better choice in reality; thus, the recovered source release history when $k = 3$ is adopted. Figure 6 displays the recovered release histories of cases 1 – 4 when $k = 3$, reflecting the recovered release histories of these cases match with the true one very well. Those results imply that the proposed approach can reconstruct the release history from an area source. In addition, the results also confirm that the best reconstruction can be obtained as the objective function has a

least value among different k.

4.3 Scenario 3: Volume Source

When contaminant is not originated from a point source but from a large less well-defined space, it may be approximated by a volume source. Scenario 3 intends to recover a volume source release history for contaminant in three-dimensional transport. The volume source dimensions are as follows: $L_1 = 0$ m and $L_2 = 5$ m for the length, $B_1 = 0$ m and $B_2 = 20$ m for the width, and $H_1 = 0$ m and $H_2 = 2$ m for the depth. Four cases are designed to assess the performance of the proposed method. For cases 1 and 2, two different aquifer configurations are considered, respectively. In case 1, the aquifer is infinite in the y-direction while for case 2 it is assumed to have a finite width of 100 m. Suppose the depth of the aquifer is 10 m and the aquifer is infinite in x-direction. The sampling concentrations are generated with the same aquifer parameters as used in scenario 1.

Because the kernel function is chosen based on the source geometry and aquifer configuration, therefore, the kernel function equals $X_2\ Y_4\ Z_2$ defined in Eqs. (9), (13), and (15) for case 1, and $X_2\ Y_2\ Z_2$ in Eqs. (9), (11), and (15) for case 2. With Eqs. (6) and (21), the spatial concentration distributions for cases 1 and 2 are calculated and shown in Fig. 7; therefore, a set of 17 sampling data is available for recovering the source release history. Figure 7 also implies that the number of source release waves

for both cases is at least two.

The unknown release history of a groundwater contaminant is represented by Eq. (22) with $3k$ unknowns. For $3k \leq 17$, the number of the terms, k, can be up to five. Hence, the trial number of release waves, k, can be from two to five. Table 1(c) lists the estimated OFV for different k in cases 1 and 2, indicating that the least OFV occurs when $k = 3$. Table 4 lists the estimated parameters determined by SA and verifies that the estimated release history function is exact when $k = 3$. Based on the obtained parameters when $k = 3$, the curve of source release history can be shown graphically. Figure 8 displays the recovered release histories of cases 1 and 2, showing that the reconstructions of both cases are in good agreement with the true one, even though the middle wave is not observed in the sampling concentration distribution. These results demonstrate that the proposed method provides a robust tool for recovering a volume source release history of a groundwater contaminant and can be applied to the cases of multi-dimensional non-point source as well.

Cases 3 and 4 are designed to investigate the impact of contaminant biodegradation on the reconstruction of case 1. Both cases consider the biodegradation rate, λ, of 0.0055 day^{-1} if the contaminant is the Trichloethene and is biodegradable under aerobic oxidation condition. We assume the λ is known in case 3 and unknown to be estimated in case 4. Figure 7 exhibits the sampling

concentrations of those two cases which consider the contaminant biodegradation. The recovered release histories for cases 3 and 4 are shown in Figure 8. In case 3 with the known λ, the source release history is reconstructed very well if compared with the true one. As for case 4, the estimated λ is 0.0039374 day^{-1} by SA with the upper and lower bounds of 0. and 0.0278 day^{-1} (Bedient et al., 1999) for λ. The source release history is recovered acceptably since the release width of the first wave is slightly underestimated and the release strength of the third wave is overestimated. The result reveals that the proposed approach also can reconstruct the source release history reasonably well if λ is unknown.

4.4 Scenario 4: Number of Monitoring Well

For spatial concentration data, a large number of monitoring wells are often needed to accurately capture the information of the plume. It implies the relative high cost involved in installing the monitoring wells. Therefore, for cost saving, scenario 4 proposes to investigate whether the proposed approach can use the temporal concentration data sampled at few wells to recover the source release history. Four cases are designed to investigate the effect of the number of the monitoring wells on the results of reconstruction of the source release history. A two-dimensional plume in an infinite aquifer from a finite area source is considered. The dimensions of the area source are assumed as 5m × 5m. The contaminant plume concentration is

calculated based on the parameter set with v = 1 m/day, D_x = 0.5 m^2/day, and D_y = 0.05 m^2/day.

The number of monitoring wells considered in cases 1 – 4 is from 4 to 1, respectively. In case 1, 4 wells are located at (40, 0), (60, 5), (80, 5), and (80, 10), and there are totally 16 sampling concentrations measured from 160 to 250 days in 30 days time increments. For case 2, three monitoring wells are placed at (40, 0), (60, 5), and (80, 10), and there are 15 concentrations sampled from 150 to 270 days in 30 days increments. Case 3 utilizes two monitoring wells located at (40, 0) and (80, 5), and considers 16 concentrations sampled from 160 to 300 days in 20 days increments. Finally, in case 4, a single monitoring well located at (40, 0) is considered, and 15 concentrations sampled from 130 to 270 days in 10 days increments are assumed. Figure 9 shows the temporal concentration data for those four cases. In sum, there are 16 sampling data for cases 1 and 3 and 15 sampling data for cases 2 and 4 to reconstruct the source release history.

Following the same recovery procedure as mentioned in Chapter 3, the value of k can be up to five in those four cases. Table 5(a) lists the estimated OFV for different k in cases 1 – 4, indicating that the objective function has a least value when k = 3, except in case 1 which has the smallest OFV when k = 4.

Table 6 lists the estimated parameters determined by SA for different k,

indicating that the estimated parameters have good accuracy when k = 3. However, in case 1 the OFV's are small when k ranges 3 to 5 and have the least value when k = 4. In case 1, when k = 4 and 5 the estimated first three parameters in Eq.(22) are close to the true ones as displayed in Table 6 and the remaining terms are near zero because the corresponding release width parameters are close to zero. Figure 10 shows the recovered release histories when k = 4 and 5 for case 1, displaying that the reconstructions match with the true one, if neglecting the spike when k = 5. This reveals that although the least OFV occurs when k = 4 for case 1, the number of the source release waves shown in Fig. 10 in fact is three. Consequently, we adopt the recovered source release function when k = 3 as the best result for case 1.

Figure 11 displays the recovered release histories of the four cases when k = 3, showing that the recovered release history for each case is in good agreement with the true one. The results demonstrate that proposed method can solve the source release history recovery problem based on temporal concentration data for the well number ranging from 1 – 4. In addition, the results indicate that the proposed method is effective since only one monitoring well with 15 sampling concentration data is good enough to solve the problem.

4.5 Scenario 5: Number of sampling data

Scenario 5 is intended to explore the minimum required numbers of temporal

concentration data for solving the source release history recovery problem. Seven cases with sampling data points of 8 to 14 are designed. One monitoring well located at (40, 0) is considered. Assume a two-dimensional plume from a finite area source while the aquifer is infinite. The dimensions of the area source and the aquifer parameters are set the same as scenario 4.

Figure 12 illustrates the data set of the seven cases that are analyzed. In case 1, there are 14 sampling concentrations measured from 147 to 251 days in 8 days increments. In case 2, totally 13 sampling concentrations are measured from 150 to 246 days in 8 days increments. Case 3 considers 12 concentrations sampled from 150 to 249 days in 9 days increments. Case 4 supposes 11 concentrations sampled from 150 to 250 days in 10 days increments. In case 5, ten sampling concentrations are measured from 150 to 249 days in 11 days increments. Case 6 considers nine concentrations sampled from 150 to 246 days in 12 days increments. Finally, in case 7, totally eight sampling concentrations are measured from 150 to 248 days in 14 days increments.

Figure 12 shows that the sampling concentration distribution with two waves for cases 1 – 7, indicating the number of source release waves, k, is two at least. Thus, the trial value of k can be from two to four in cases 1 – 3, from two to three in cases 4 – 6, and should be two in case 7. Table 5(b) lists the OFV for different k of each

case, indicating that the least OFV is obtained when $k = 3$ in cases 1 – 6. Notice that the OFV for $k = 3$ is at least four orders less than those for $k = 2$ and 4 in cases 1 – 3; and six orders less than those for $k = 2$ in cases 4 – 6. Hence, the best recovered release history can be obtained when $k = 3$. As for case7, the source release history could merely be reconstructed based on the estimated parameters when $k = 2$.

Table 7 shows the best possible parameters of the assumed release function for $k = 3$ in cases 1 – 6 and for $k = 2$ in case 7. The result demonstrates that the estimated parameters listed in Table 7 are in good accuracy, except in case 7. The reconstruction in case 7 is a two-wave source release history; however, the true source release history has a three-wave curve. Such a problem could attribute to the fact that the number of the sampling data in case 7 is insufficient to identify the value of k. So the required number of sampling data in this case study has to be more than or equal to nine.

4.6 Scenario 6: A Guideline for Sampling

Based on previous studies, good reconstructions rely on the sampling concentration data that capture adequate information of the spreading plume. However, how do we assure that the sampled concentrations are good enough for recovering the source release history? To answer this question, scenario 6 attempts to establish a general guideline to allow us in making appropriate sampling for

recovering a source release history. Eleven cases are designed to draw the guideline on sampling region and sampling period for a two-dimensional plume in an infinite aquifer from an area source. The aquifer parameters are set the same as scenario 4.

Seven cases are designed to investigate the effect of the monitoring well location on the result of recovering the source release history since the monitoring well may not locate right at the downgradient of the source. The area source dimensions are as follows: L_1 = 0 m and L_2 = 5 m for the length, B_1 = 0 m and B_2 = 5 m for the width. The monitoring wells in cases 1 – 7 are considered to be installed at (40, 5), (40, 6), (40, 7), (40, 8), (40, 9), (40, 10), and (40, 11), respectively. The sampling period for those cases ranges from 150 to 249 days with 9 days time increments. Table 8 shows 12 temporal concentrations in cases 1 – 7.

Table 5(c) lists the OFV for different k, presenting that the objective function has a least value when k = 3 for all cases. Hence, we conclude that the best recovered release history is obtained when k = 3. Notice that the OFV for k = 3 is at least four orders less than those for k = 2 and 4 in case 1, revealing that a higher plume concentration level at the monitoring well tends to give a more obvious difference in OFV for different k. On the other hand, as the monitoring well deviates from the center line of the plume (y = 2.5 m) more than 8 m (case 7), the difference in OFV for different k is insignificant.

Table 9 presents the parameters of the assumed release function for cases 1 – 7 when k = 3, indicating the source release histories of cases 1 – 6 are correctly recovered; while the reconstruction of case 7, with the monitoring well located more than 8 m from the center line of the plume in y-direction, is inaccurate. In case 7, the three waves are out of shape since the estimated source release time has moderate shift. The results indicate that sampling concentrations measured within 8 m from the center line of the plume can be used to recover a source release history.

Due to plume concentrations can be described by Gaussian distribution in 1-D, 2-D, or 3-D geometries, and the spread of the plume can be determined based on the dispersion coefficients, $\sigma^2 = 2Dt_{evol}$, where t_{evol} is the plume evolution time (Bedient et al., 2003). Hence, one standard deviation of the contaminant distribution in y-direction in this case study, $\sigma_y = \sqrt{2D_y t_{evol}}$, ranges from 4.1 to 4.8 m. Accordingly, the position of 8 m deviated from the center line of the plume in y-direction is about $1.96\sigma_y$. Therefore, the proper sampling region is suggested to be within the area covered by $\pm 1.96\sigma_y$ from the center of the plume.

Cases 8 – 10 are designed to investigate the impact of sampling period on the reconstruction of the source release history. The monitoring well is located at (40, 0). There are 12 sampling data are used. In case 8, the sampling period is between 147 and 249 days. Figure 13(a) illustrates the concentration data set while Fig. 13(b)

shows the recovered release history. The plots reveal that as the whole plume concentration is observed, though the peak of the concentration curve is not sampled, the reconstructed release history is still in good agreement with the true release history.

In case 9, sampling concentrations are taken with a uniform interval of 7 days between 153 and 230 days. The sampling period only covers the early part of the temporal concentration distribution curve observed at the monitoring well. Figure 14(a) displays the temporal concentrations distribution, showing that the latter part of the concentration curve is not sampled. Figure 14(b) exhibits the recovered release history obtained based on the sampling data, indicating that the source release history is reconstructed very well if compared with the true one. The result shows that even though the sampling data does not cover the whole distribution, the source release history can still be reconstructed very well.

In case 10, sampling concentrations are taken from 148 to 225 days with 7 days time increment. The sampling period is shifted about 5 days earlier than that in case 9. Figures 15(a) and 15(b) display the sampling concentrations and the recovered release history, respectively. The result reveals that in case 10 sampling data does not cover the latter part of the plume concentration, as case 9 does, and gets poor result in the third release wave of source release history. Such a problem may

attribute to the problem that the falling part of the third wave is not included in case 10. If both the rising and falling parts of data for a concentration wave are sampled, the source release curve is reconstructed correctly, no matter the peak concentration of the plume is included or not.

Case 11 is designed to prove the guideline on sampling period. Suppose there are four parties, A, B, C, and D, who are potentially responsible for a groundwater contamination and both B and D really produce the contamination. Party A owned the site for the first 100 days, party B hold the second 100 days, party C owned the third 100 days, and party D had the last 100days. Thus, the time of those four parties possessed the site ranges from the first day to 400 days. Assume that a monitoring well is located at (200, 0) and the average linear velocity is 1 m/day. Accordingly, the appropriate sampling period may range from 180 days to 620 days for the monitoring well, if both the advective and dispersive transports are considered.

Figure 16(a) shows the sampling concentrations measured with a uniform interval of 20 days. Totally 23 sampling data are available to solve the source release history recovery problem using the proposed approach. Figure 16(b) displays the curve of the recovered source release history of the groundwater contamination, indicating that there are two release waves occurred at 130 days and 340 days. Thus, the parties B and D are identified who owned the site at these two

specific times. This result confirms that the proposed method can successfully identify the ones who should take the responsibility for the contamination.

Based on the results of those case studies, a guideline on sampling region and sampling period can be drawn as: (1) the sampling concentrations measured within the extend of $1.96\sigma_y$ from the mean of the plume can be used to recover the source release history; (2) proper sampling period could be estimated by considering the contaminant transport mechanisms; however, both the rising and falling parts of data for a concentration wave should be sampled, the source release curve can then be reconstructed correctly, no matter the peak concentration of the plume is measured or not.

4.7 Scenario 7: Guideline Verification

The guideline drawn in scenario 6 relies on the temporal concentration data and scenario 7 is to demonstrate that the guideline is also applicable for analyzing the spatial concentration data. Consider a one-dimensional point source located at $x = 0$ with v and D_x being equal to 1 m/day and 1 m^2/day, respectively. Five cases are designed to assess the applicability of the proposed method with different sampling time. Suppose the suspicious parties possessed the site between 130 days and 190 days. The sampling time in cases 1 – 5 is respectively at 225, 300, 450, 600, and 900 days. The distance of the plume migrates from the source ranges between 35 and 95

m in case 1, 110 and 170 m in case 2, 260 and 320 m in case 3, 410 and 470 m in case 4, and 710 and 770 m in case 5. Hence, the spread of the contaminant plume in each case is roughly portrayed.

In x-direction, the region of 1.96σ is calculated by $1.96\sigma_x = 1.96\sqrt{2D_x t_{evol}}$. For case 1, the region ranges from 19 m ($35 - 1.96\sqrt{2\times1\times35}$) to 122 m ($95 + 1.96\sqrt{2\times1\times95}$). Similarly, the region ranges from 81 m to 206 m for case 2, from 216 m to 369 m for case 3, from 354 m to 530 m for case 4, and from 637 m to 846 m for case 5. Consider 12 spatial concentration data measured within the region estimated above. Figure 17 shows the spatial concentration data for each case, revealing that a curve with two waves is exhibited in both cases 1 and 2, and a single-wave curve is displayed in cases 3 – 5. The result demonstrates that the mixing and spreading phenomenon of the plume increases with time.

Since 12 sampling concentrations are available, the value of k can be up to 4. The best k could be obtained while the objective function has a least value. Table 1(d) lists the OFV for different k in each case, indicating that the least OFV occurs when $k = 3$. The OFV for $k = 3$ is at least two orders less than those for $k = 2$ and 4 in cases 1 and 2 and about one order less in case 3. While for cases 4 and 5 (plume evolution time beyond 410 days), the OFV for different k is almost the same.

Figure 18 shows the recovered source release history of cases 1 – 5 when $k = 3$.

In cases 1 and 2, the reconstructions give very good fit to the true one, except that the second release wave in case 2 is somewhat overestimated. As for case 3, even though the shape of three release waves is not high in sampling concentrations, the recovered source release history is still close to the true release history except the second wave is slightly overestimated. In case 4, the middle and the third release waves are overestimated. For case 5, the middle wave is absent and the third wave is overestimated. These results indicate that the sampling concentration data obtained about 320 days after the source release still give a nice reconstruction as compared with the true source release history. In addition, the results confirm that the guideline on sampling region established in scenario 6 is applicable to the spatial concentration data.

4.8 Scenario 8: Measurement errors

Due to the lack of precision in the measurement devices, field sampled concentration usually contains measurement error, which may be expressed as:

$$C_{meas}(x_n,T) = C_{ext}(x_n,T) + \varepsilon\delta_n C_{ext}(x_n,T) \tag{24}$$

where $C_{meas}(x_n,T)$ is the measured concentration at location x_n at time T, $C_{ext}(x_n,T)$ is the exact concentration at location x_n at time T, x_n is the location of the nth sample, ε is the error magnitude, δ_n is a random number from a Gaussian standard population, and the product $\varepsilon\delta_n$ is equal to the relative measurement error at x_n.

Three cases with different error levels are studied. Case 1 considers a very small measurement error, i.e., $\varepsilon = 0.01$; case 2 evaluates an acceptable level of inaccuracy for $\varepsilon = 0.05$; and case 3 assumes an error with $\varepsilon = 0.1$. Suppose a one-dimensional point source located at $x = 0$, with v and D_x, being equal to 1 m/day and 1 m^2/day, respectively. The time of sampling is at 225 days. Twelve spatial concentrations sampled within the region of 95 % of contaminant mass are considered. The concentrations with three different levels of measurement error are shown in Fig. 19.

Table 1(e) lists the OFV for different k of each case, indicating that the least OFV occurred when $k = 3$. Therefore, the best recovered release history is obtained when $k = 3$. Notice that the OFV for $k = 3$ is at least one orders less than those for $k = 2$ and 4 in each case, revealing that the presence of different error levels in concentration data does not affect the selection of k.

The recovered source release histories when $k = 3$ in each case are shown in Fig. 20. In case 1 with a small error of $\varepsilon = 0.01$, the source release history is recovered acceptably, though the first and the second waves is overestimated. In case 2 with an error of $\varepsilon = 0.05$, the release strength of the source is estimated too high, in addition, the middle wave is disappeared. In case 3 with a larger error of $\varepsilon = 0.1$, the release strength of the first wave is incorrect and the middle wave is also disappeared. Results indicate that the accuracy of a recovered source release history strongly depends on the

precision of the sampling concentrations. Although the proposed approach is sensitive to measurement error, it still can solve the source release times reasonably well, even when the measurement error is significant.

4.9 Scenario 9: Two Adjacent Point Sources

Consider an aquifer was polluted by two different contaminant sources at known spots within an area where the landlord changed several times in the past. Therefore, the objective of scenario 9 is to investigate whether the proposed method can distinguish the contamination proportions between two adjacent sources if sampling data are few. In addition, the effects of the location of monitoring wells and the degree of dispersion on the result of recovering release history are also studied.

Suppose the contaminant is released from two point sources into a two-dimensional homogeneous aquifer and the two independent point sources are located at $P_1(x_1, y_1)$ and $P_2(x_2, y_2)$. Due to the linearity of the ADE, the plume concentration in the aquifer can be expressed as (Butera and Tanda, 2003):

$$C(x, y, T) = \sum_{i=1}^{2} \int_{0}^{T} C_{ini}(\tau) F(x - x_i, y - y_i, T - \tau) d\tau \qquad (25)$$

where $C_{ini}(\tau)$ is the ith contaminant source release function at the inlet boundary [ML^{-3}], x_i and y_i are the x and y coordinates of the ith plume source. The kernel function $F(x - x_i, y - y_i, T - \tau)$ equals $X_1 Y_3$ in Eqs. (8) and (12).

An example is used to demonstrate the applicability of the proposed method in solving a release history recovery problem with two contaminant sources. The example supposes that two independent point sources located at $P_1(0, 0)$ and $P_2(6, 6)$ and the contaminant is conservative. The "true" release history of the first source is assumed as (Skaggs and Kabala, 1994)

$$C_{in1}(t) = \exp\left(-\frac{(t-130)^2}{50}\right) + 0.3\exp\left(-\frac{(t-150)^2}{200}\right) + 0.5\exp\left(-\frac{(t-190)^2}{98}\right) \quad (26)$$

while that of the second source is:

$$C_{in2}(t) = 0.5\exp\left(-\frac{(t-200)^2}{50}\right) + 0.3\exp\left(-\frac{(t-230)^2}{200}\right) + \exp\left(-\frac{(t-260)^2}{98}\right) \quad (27)$$

Three cases are designed to assess the performance of the proposed method and the impacts of the location of monitoring wells and the degree of the dispersion on the estimated results. Consider two monitoring wells, MWs 1 and 2. In case 1, MWs 1 and 2 are located at (50, 0) and (50, 6), respectively. The sampling concentrations are calculated with the parameters v = 1 m/day, D_x = 1 m^2/day, and D_y = 0.1 m^2/day. In case 2, the locations of MWs 1 and 2 are respectively installed at (300, 0) and (300, 6); however, the sampling concentrations are still calculated with the same parameters as used in case 1. In case 3, the monitoring well locations and the parameters are the same as case 2 except D_x = 0.1 m^2/day. The sampling concentrations at MWs 1 and 2 are simulated using Eqs. (25), (26), and (27).

The sampling concentration distributions for those three cases are shown in Fig. 21, exhibiting the effect of the well location and the dispersion phenomena on the sampling data. The plume concentration levels at MWs 1 and 2 in case 1 are higher than those of case 2. This reveals that a shorter distance between the monitoring well and the contaminant source tends to give a higher concentration level at the monitoring well. In addition, the peaks of the concentration distribution in case 3 with D_x = 0.1 m^2/day are higher than those in case 2 with D_x = 1 m^2/day. Accordingly, a higher dispersion coefficient signifies a more smearing plume shape. The result indicates that dispersion smears the plume distribution and this effect increases with the distance between the monitoring well and the source.

The concentration data in case 1 are measured from 170 days to 335 days with a uniform interval of 15 days. In case 2, the data are sampled from 380 days to 600 days with an interval of 20 days. In case 3, the data are taken from 410 days to 575 days with an interval of 15 days. There are totally 24 sampling data available for each case to recover the two source release histories. Notice that a larger spreading plume leads to a longer sampling period and interval for maintaining the total number of sampling data unchanged.

The unknown release histories of two point sources are assumed in an exponential form of Eq. (22); accordingly, totally 3*k* unknowns have to be determined

by SA with 24 sampling concentrations. Figure 21 shows the sampling concentration distributions with three waves at MWs 1 and 2 for cases 1 – 3. Therefore, those curves suggest to use $k = 3$ in estimating the release functions for each case. Figure 22 shows the recovered release histories of cases 1 – 3. In case 1, the estimated release histories of sources 1 and 2 are fairly close to the true ones, though the third wave of the source 1 and the first wave of the source 2 are slightly overestimated. In case 2, the middle wave of sources 1 and 2 is not recovered because the information of the middle wave associated with the sampling data is diminished at the distance of 300 m between the source and the monitoring well. As in case 3, although the location of the monitoring well is similar to that of case 2, the release histories of sources 1 and 2 are reconstructed very well owing to the fact that the dispersion coefficient in case 1 is smaller than that of case 2. These results indicate that the proposed method can recognize the release histories of two adjacent sources based on 24 sampling concentrations. In addition, the results also confirm the importance of the location of the monitoring well and the degree of dispersion in the release history recovery problem.

CHAPTER 5 CONCLUSIONS

An approach using a function-fitting technique and SA incorporated with a fundamental solution of the groundwater transport equation is developed to recover the source release history of a groundwater contaminant. Case studies include the problems in one-, two-, and three- dimensions, three types of contaminant source geometries, and two kinds of aquifer configurations. The source geometries include point, area, and volume sources. The aquifer configurations contain both infinite aquifer and finite width aquifer. Topics of measurement errors, contaminant biodegradation, the degree of dispersion, the location of monitoring well, the number of sampling data, the use of temporal concentration data or spatial concentration data, and the existence of two contaminated sources are also investigated. In addition, a guideline for the optimal sampling strategy in reconstructing the source release history is suggested. Five conclusions can be drawn as follows:

First, the proposed method can be applied to a one-dimensional point source case and multi-dimensional non-point source cases as well even if the contaminant biodegradation rate is unknown. In addition, the proposed method can also deal with the problem of the contamination proportions from two adjacent sources.

Second, this study shows that one monitoring well with nine sampling concentrations is enough to solve the recovery problem of source release history with

three sinuous waves. This implies that the proposed method is very cost-effective in terms of number of monitoring wells used in recovering the release history.

Third, although the proposed approach is sensitive to the measurement error, it still can solve the source release times reasonably well, even when the measurement error is significant.

Forth, a guideline on sampling region and sampling period can be drawn as: (1) samples measured within the extend of 1.96σ from the mean of the plume are suitable to recover the source release history; (2) proper sampling period can be estimated by considering the contaminant transport mechanism; however, both the rising and falling parts of data for a concentration wave should be sampled, the source release curve can then be reconstructed correctly, no matter the peak concentration of the plume is measured or not.

Fifth, high dispersion coefficient and large monitoring distance will result in low concentration detected in the monitoring well and poor recovered history. Therefore, it is to suggest that the monitoring wells should be installed close to the source for better results in recovering the source release history.

REFERENCES

Alapati, S., and Z. J. Kabala (2000), Recovering the release history of a groundwater contaminant via the non-linear least-squares estimation, *Hydrol. Process*, 14, 1003-1016.

Atmadja, J., and A. C. Bagtzoglou (2001), State of the Art Report on Mathematical Methods for Groundwater Pollution Source Identification, *Environ. Forens*. 2, 205-214.

Bedient, P. B., Rifai, H. S., and Newll, C. J. (1999), Ground Water Contaminant, 2nd ed., PTR Prentice Hall.

Boano, F., R. Revelli, and L. Ridolfi (2005), Source identification in river pollution problems: a geostatistical approach, *Water Resour. Res.*, 41, W07023.

Butcher, J. B., and T. D. Gauthier (1994), Estimation of residual dense NAPL mass by inverse modeling, *Ground water*, 32, 71-78.

Butera, I., and M.G. Tanda (2003), A geostatistical approach to recover the release history of groundwater pollutants, *Water Resour. Res.*, 39(12), 4-1-4-9.

Kirkpatrick, S., C.D. Gelatt Jr., and M.P. Vecchi (1983), Optimization by Simulated Annealing. *Science*, 220 (4598), 671-680.

Lin, B. H. (1999), Fitting the term structure of interest rates for Taiwanese government bonds, *Journal of Multinational Financial Management*, 9, 331–352.

Pham, D. T. and D. Karaboga (2000), Intelligent Optimi sation Techniques, Springer, Great Britain.

Press, W. H., B. P. Flannery, S. A. Teukolsky, and W. T. Vetterling (1986), Numerical Recipes: The art of scientific computing, NY: Cambridge University Press.

Skaggs, T.H., and Z.J. Kabala (1994), Recovering the release history of a groundwater contaminant, *Water Resour. Res.*, 30(1), 71-79.

Skaggs, T.H., and Z.J. Kabala (1995), Recovering the history of a groundwater contaminant plume: Method of quasi-reversibility, *Water Resour. Res.*, 31(11), 2669-2673.

Skaggs, T.H., and Z.J. Kabala (1998), Limitations in recovering the history of a groundwater contaminant plume, *Journal of Contaminant Hydrology.*, 33,

347-359.

Todd, D. K. and L. W. Mays (2005), Groundwater Hydrology, 3rd ed., John Wiley &Sons, NY.

Wagner, B. J. (1992), Simultaneously parameters estimation and contaminant source characterization for coupled groundwater flow and contaminant transport modeling, *J. Hydro*., 135, 275-303.

Woodbury, A., E. Sudicky, T.J. Ulrych and R. Ludwig (1998), Three-dimensional plume source reconstruction using minimum relative entropy inversion, *Journal of Contaminant Hydrology,* 32*,* 131-158.

Yeh, G. H. (1981), AT123D: Analytical transient one-, two-, and three-dimensional simulation of waste transport in the aquifer system, *Report ORNL-5602, Oak Ridge, Tennessee.*

Table 1. The OFV for different *k* based on spatial concentration data.

	OFV				
k	Case 1	Case 2	Case 3	Case 4	Case 5
	(a) Scenario 1: a point source				
2	1.62×10^{-3}	1.37×10^{-5}	1.22×10^{-6}	7.68×10^{-4}	7.23×10^{-3}
3	$\mathbf{1.79\times10^{-6}}$	$\mathbf{4.05\times10^{-7}}$	$\mathbf{5.17\times10^{-7}}$	$\mathbf{5.02\times10^{-7}}$	$\mathbf{5.45\times10^{-7}}$
4	1.77×10^{-5}	4.23×10^{-7}	5.74×10^{-7}	2.34×10^{-6}	5.76×10^{-7}
5	2.24×10^{-5}	4.57×10^{-7}	6.41×10^{-7}	3.27×10^{-6}	5.91×10^{-7}
	(b) Scenario 2: an area source				
2	5.50×10^{-3}	6.13×10^{-4}	1.40	2.46×10^{-3}	-
3	$\mathbf{2.04\times10^{-6}}$	$\mathbf{7.92\times10^{-7}}$	$\mathbf{1.03\times10^{-6}}$	$\mathbf{8.13\times10^{-7}}$	-
4	$\mathbf{1.62\times10^{-6}}$	1.12×10^{-6}	5.65×10^{-4}	2.62×10^{-5}	-
5	3.87×10^{-6}	1.20×10^{-5}	4.50×10^{-4}	1.85×10^{-4}	-
	(c) Scenario 3: a volume source				
2	1.31×10^{-3}	5.29×10^{-3}	-	-	-
3	$\mathbf{2.45\times10^{-6}}$	$\mathbf{2.71\times10^{-6}}$	-	-	-
4	2.68×10^{-5}	1.96×10^{-5}	-	-	-
5	5.51×10^{-5}	1.59×10^{-4}	-	-	-
	(d) Scenario 7: guideline verification				
2	9.15×10^{-4}	3.85×10^{-5}	1.91×10^{-5}	1.15×10^{-6}	3.98×10^{-6}
3	$\mathbf{7.62\times10^{-6}}$	$\mathbf{4.35\times10^{-7}}$	$\mathbf{4.99\times10^{-7}}$	$\mathbf{1.012\times10^{-7}}$	$\mathbf{3.42\times10^{-7}}$
4	4.49×10^{-4}	1.34×10^{-4}	3.30×10^{-6}	1.013×10^{-7}	4.91×10^{-7}
	(e) Scenario 8: measurement errors				
2	3.21×10^{-1}	9.98×10^{-1}	9.07×10^{-1}	-	-
3	$\mathbf{5.02\times10^{-3}}$	$\mathbf{3.48\times10^{-3}}$	$\mathbf{3.04\times10^{-3}}$	-	-
4	3.37×10^{-2}	1.21×10^{-2}	1.09×10^{-2}	-	-

Table 2. Scenario 1: estimated parameters in the assumed release function for different k.

k	the release strength a_j					the release times t_j					the release width parameters σ_j				
	1	2	3	4	5	1	2	3	4	5	1	2	3	4	5
						True $C_{in}(t)$									
	1.00	**0.30**	**0.50**			**130.00**	**150.00**	**190.00**			**5.00**	**10.00**	**7.00**		
						Estimated $C_{in}(t)$ for Case 1									
2	0.68	0.46				135.61	188.97				11.54	8.29			
3	***1.00***	***0.30***	***0.50***			***130.55***	***152.03***	***189.93***			***5.43***	***8.43***	***7.07***		
4	1.14	2.83	0.51	78.89		130.86	152.08	190.49	171.78		5.05	0.55	6.63	0.23	
5	3.30	8.68	0.50	32.83	90.39	128.60	156.62	190.09	146.27	166.68	1.42	0.38	6.91	0.34	0.25
						Estimated $C_{in}(t)$ for Case 2									
2	0.64	0.48				135.67	189.38				12.37	7.66			
3	***0.85***	***0.32***	***0.50***			***129.20***	***146.06***	***190.17***			***4.84***	***12.38***	***6.98***		
4	0.83	0.27	0.50	79.64		130.15	149.48	190.21	162.12		5.99	11.13	6.94	0.08	
5	0.67	0.28	0.50	0.34	35.58	129.52	148.53	190.20	121.43	135.91	5.52	11.55	6.96	1.05	0.13
						Estimated $C_{in}(t)$ for Case 3									
2	0.63	0.51				135.10	189.13				12.66	7.29			
3	***0.76***	***0.24***	***0.52***			***131.93***	***156.02***	***189.58***			***5.99***	***8.69***	***6.86***		
4	2.51	0.39	0.51	2.25		130.23	138.96	189.82	88.49		0.87	15.04	6.81	0.21	
5	40.85	0.54	0.50	94.29	52.95	124.83	138.79	191.48	179.21	203.54	0.17	11.72	5.85	0.08	0.14

Estimated $C_{in}(t)$ for Case 4

2	0.55	62.49				136.84	191.48				15.85	0.37			
3	***1.02***	***0.32***	***0.49***			***129.39***	***145.54***	***190.07***			***3.92***	***12.56***	***7.02***		
4	0.85	22.82	0.50	74.97		133.33	160.80	189.88	123.34		8.10	0.11	7.09	0.19	
5	1.12	0.33	0.50	80.76	1.84	129.38	145.20	190.71	91.49	211.59	3.43	12.80	6.94	0.23	0.27

Estimated $C_{in}(t)$ for Case 5

2	0.66	0.51				133.86	187.45				11.98	7.59			
3	***1.11***	***0.39***	***0.53***			***129.05***	***151.96***	***187.93***			***5.21***	***5.53***	***7.08***		
4	1.18	5.85	0.53	73.20		129.33	151.73	187.90	163.38		5.04	0.50	7.10	0.25	
5	1.29	4.05	0.53	36.02	11.84	129.94	153.50	187.80	149.80	107.74	4.56	0.64	7.16	0.08	0.08

Table 3. Scenario 2: estimated parameters in the assumed release function for different k.

k	the release strength a_j					the release times t_j					the release width parameters σ_j				
	1	**2**	**3**	**4**	**5**	**1**	**2**	**3**	**4**	**5**	**1**	**2**	**3**	**4**	**5**
						True $C_{in}(t)$									
	1.00	**0.30**	**0.50**			**130.00**	**150.00**	**190.00**			**5.00**	**10.00**	**7.00**		
						Estimated $C_{in}(t)$ for Case 1									
2	0.67	0.46				135.63	189.05				11.80	8.12			
3	***1.00***	***0.30***	***0.50***			***130.37***	***151.42***	***189.96***			***5.29***	***9.06***	***7.04***		
4	0.97	0.29	0.47	0.41		129.82	148.63	190.85	183.93		4.81	11.68	6.67	0.77	
5	158.15	0.31	0.50	135.09	112.50	126.91	146.33	190.10	137.88	105.87	0.21	12.37	6.94	0.12	0.08
						Estimated $C_{in}(t)$ for Case 2									
2	0.66	0.47				135.64	189.07				11.88	7.93			
3	***0.99***	***0.30***	***0.50***			***130.16***	***150.58***	***189.96***			***5.21***	***9.58***	***7.00***		
4	149.65	0.34	0.50	211.86		127.02	144.33	190.08	134.11		0.17	13.03	6.92	0.10	
5	0.87	219.69	0.50	59.97	92.02	133.03	154.89	189.79	158.93	6.74	7.74	0.11	7.10	0.19	0.07
						Estimated $C_{in}(t)$ for Case 3									
2	52.31	0.30				133.10	182.55				0.29	18.09			
3	***1.00***	***0.30***	***0.50***			***130.00***	***150.01***	***190.00***			***5.00***	***9.99***	***7.00***		
4	1.81	0.34	0.50	34.10		129.58	144.66	190.10	115.11		1.93	12.82	6.91	0.15	
5	4.39	0.34	0.50	224.99	40.36	130.15	144.87	190.08	119.68	209.54	0.64	12.70	6.89	0.07	0.03
						Estimated $C_{in}(t)$ for Case 4									
2	0.66	0.47				135.68	189.09				11.88	7.95			
3	***0.98***	***0.29***	***0.50***			***130.20***	***150.64***	***190.01***			***5.26***	***9.69***	***7.00***		
4	0.92	3.53	0.50	61.08		132.62	158.38	189.71	199.11		7.15	0.58	7.23	52.06	
5	0.81	164.72	0.51	217.47	20.82	133.81	149.64	190.08	162.04	192.31	8.71	138.52	6.88	0.14	0.11

Table 4. Scenario 3: estimated parameters in the assumed release function for different k.

k	the release strength a_j					the release times t_j					the release width parameters σ_j				
	1	**2**	**3**	**4**	**5**	**1**	**2**	**3**	**4**	**5**	**1**	**2**	**3**	**4**	**5**
						True $C_{in}(t)$									
	1.00	**0.30**	**0.50**			**130.00**	**150.00**	**190.00**			**5.00**	**10.00**	**7.00**		
						Estimated $C_{in}(t)$ for Case 1									
2	0.66	0.47				135.71	189.20				12.09	7.82			
3	***0.95***	***0.30***	***0.50***			***129.72***	***148.33***	***190.07***			***4.86***	***11.16***	***6.96***		
4	1.62	0.41	0.31	1.12		128.22	146.71	188.20	192.38		5.07	10.72	9.06	0.20	
5	3.55	0.36	0.50	101.63	172.48	128.75	143.92	190.03	68.34	93.26	1.15	10.99	6.99	0.05	0.18
						Estimated $C_{in}(t)$ for Case 2									
2	0.66	0.47				135.70	189.18				12.08	7.83			
3	***0.99***	***0.29***	***0.50***			***130.70***	***152.46***	***189.84***			***5.59***	***8.44***	***7.04***		
4	11.173	0.35	0.50	37.74		129.84	142.80	190.16	166.43		0.31	14.01	6.90	11.59	
5	10.37	0.33351	0.50	205.70	62.50	131.05	142.22	190.30	17.06	194.19	0.43	15.17	6.80	112.10	60.99

Table 5. The OFV for different *k* based on temporal concentration data.

	OFV						
k	Case 1	Case 2	Case 3	Case 4	Case5	Case 6	Case 7
	(a) Scenarios 4: number of monitoring well						
2	7.09×10^{-2}	8.58×10^{-2}	1.17×10^{-2}	1.90×10^{-1}	-	-	-
3	**4.12×10^{-7}**	**1.41×10^{-6}**	**1.09×10^{-6}**	**6.82×10^{-7}**	-	-	-
4	**3.74×10^{-7}**	9.59×10^{-6}	3.35×10^{-6}	4.13×10^{-4}	-	-	-
5	4.29×10^{-7}	5.90×10^{-6}	4.27×10^{-4}	2.08×10^{-4}	-	-	-
	(b) Scenarios 5: number of sampling data						
2	0.249	0.247	0.221	0.189	0.153	0.131	0.244
3	**4.03×10^{-7}**	**1.49×10^{-7}**	**3.74×10^{-7}**	**5.24×10^{-7}**	**7.23×10^{-7}**	**5.20×10^{-7}**	**-**
4	7.29×10^{-3}	8.12×10^{-3}	3.05×10^{-3}	-	-	-	-
	(c) Scenarios 6: guideline on sampling region						
2	0.221	8.17×10^{-2}	2.04×10^{-2}	3.41×10^{-3}	3.56×10^{-4}	3.19×10^{-5}	1.58×10^{-6}
3	**2.74×10^{-7}**	**6.97×10^{-8}**	**1.73×10^{-7}**	**7.84×10^{-8}**	**9.55×10^{-8}**	**1.46×10^{-7}**	**1.94×10^{-7}**
4	5.24×10^{-3}	1.02×10^{-7}	1.83×10^{-7}	4.20×10^{-7}	1.46×10^{-7}	2.67×10^{-7}	2.35×10^{-7}

Table 6. Scenario 4: estimated parameters in the assumed release function for different k.

k	the release strength a_j					the release times t_j					the release width parameters σ_j				
	1	**2**	**3**	**4**	**5**	**1**	**2**	**3**	**4**	**5**	**1**	**2**	**3**	**4**	**5**
						True $C_{in}(t)$									
	1.00	**0.30**	**0.50**			**130.00**	**150.00**	**190.00**			**5.00**	**10.00**	**7.00**		
						Estimated $C_{in}(t)$ for Case 1									
2	0.72	0.41				134.70	189.04				11.06	9.84			
3	***1.00***	***0.30***	***0.50***			***130.01***	***150.03***	***189.99***			***5.00***	***9.98***	***6.98***		
4	1.00	0.30	0.50	91.61		130.00	150.03	190.00	200.08		5.00	9.98	6.98	0.004	
5	1.00	0.30	0.50	81.99	23.59	130.01	150.07	189.99	1.16	213.46	5.01	9.95	6.98	0.55	0.001
						Estimated $C_{in}(t)$ for Case 2									
2	0.66	0.41				133.97	188.82				10.61	8.89			
3	***0.96***	***0.33***	***0.51***			***129.21***	***145.59***	***190.11***			***4.03***	***12.46***	***6.87***		
4	2.20	0.36	0.49	96.17		129.38	143.38	190.01	112.86		1.50	12.96	7.06	0.09	
5	1.07	0.25994	0.50	14.80	11.05	130.68	158.96	189.91	147.30	171.05	5.29	4.94	7.07	0.09	0.12
						Estimated $C_{in}(t)$ for Case 3									
2	0.99	0.30				132.05	182.50				6.66	16.79			
3	***0.99***	***0.30***	***0.50***			***130.13***	***150.60***	***189.98***			***5.18***	***9.51***	***7.00***		
4	0.99	0.30	0.50	86.78		130.21	150.99	189.97	160.99		5.30	9.17	7.00	0.14	
5	0.90	94.65	0.50	15.44	48.43	131.94	154.07	189.82	15.24	19.13	7.24	0.13	7.09	1.03	1.97
						Estimated $C_{in}(t)$ for Case 4									
2	0.74	0.42				133.98	188.90				10.34	9.31			
3	***1.00***	***0.30***	***0.50***			***130.01***	***150.02***	***190.00***			***5.00***	***9.98***	***7.00***		
4	3.76	0.34	0.50	36.88		129.09	143.55	190.17	141.34		0.91	13.87	6.81	0.24	
5	30.05	0.37	0.49	98.96	98.55	128.66	142.31	190.20	164.83	183.71	0.41	13.03	6.90	0.11	0.20

Table 7. Scenario 5: the best possible parameters of source release function.

k	the release strength a_j			the release times t_j			the release width parameters σ_j		
	1	**2**	**3**	**1**	**2**	**3**	**1**	**2**	**3**
				True $C_{in}(t)$					
	1.00	**0.30**	**0.50**	**130.00**	**150.00**	**190.00**	**5.00**	**10.00**	**7.00**
				Estimated $C_{in}(t)$ for Case 1					
3	1.00	0.30	0.50	130.00	150.00	190.00	5.00	10.02	6.99
				Estimated $C_{in}(t)$ for Case 2					
3	1.00	0.30	0.50	129.99	149.97	190.01	4.99	10.01	7.00
				Estimated $C_{in}(t)$ for Case 3					
3	1.00	0.30	0.50	130.01	150.05	190.00	5.01	9.98	7.00
				Estimated $C_{in}(t)$ for Case 4					
3	1.00	0.30	0.50	130.00	149.99	190.00	5.00	10.00	7.00
				Estimated $C_{in}(t)$ for Case 5					
3	1.00	0.30	0.50	130.00	149.99	190.00	5.00	10.00	7.00
				Estimated $C_{in}(t)$ for Case 6					
3	1.00	0.30	0.50	129.99	149.96	190.01	5.00	10.05	7.00
				Estimated $C_{in}(t)$ for Case7					
2	28.14	0.25	-	133.05	178.79	-	0.31	27.22	-

Table 8. Scenario 6: the sampling concentration data for cases 1 – 7.

Time	Sampling concentrations in the monitoring well						
(days)	Case 1 (40,5)	Case 2 (40,6)	Case 3 (40,7)	Case 4 (40,8)	Case 5 (40,9)	Case 6 (40,10)	Case 7 (40,11)
150.0	0.094	0.052	0.022	0.007	0.002	0.000	0.000
159.0	0.852	0.495	0.229	0.083	0.024	0.005	0.001
168.0	1.675	1.018	0.507	0.204	0.066	0.017	0.004
177.0	1.209	0.754	0.392	0.168	0.060	0.017	0.004
186.0	0.779	0.483	0.248	0.105	0.037	0.011	0.003
195.0	0.544	0.339	0.175	0.075	0.026	0.008	0.002
204.0	0.286	0.179	0.094	0.041	0.015	0.005	0.001
213.0	0.319	0.189	0.091	0.036	0.011	0.003	0.001
222.0	0.767	0.459	0.222	0.086	0.027	0.007	0.001
231.0	0.867	0.535	0.273	0.114	0.039	0.011	0.002
240.0	0.414	0.264	0.142	0.064	0.024	0.007	0.002
249.0	0.094	0.062	0.035	0.017	0.007	0.002	0.001

Table 9. Scenario 6: the best parameters of source release function.

k	the release strength a_j			the release times t_j			the release width parameters σ_j		
	1	**2**	**3**	**1**	**2**	**3**	**1**	**2**	**3**
				True $C_{in}(t)$					
	1.00	**0.30**	**0.50**	**130.00**	**150.00**	**190.00**	**5.00**	**10.00**	**7.00**
				Estimated $C_{in}(t)$ for Case1					
3	1.00	0.30	0.50	130.00	150.00	190.00	5.00	10.02	7.00
				Estimated $C_{in}(t)$ for Case 2					
3	1.00	0.30	0.50	130.01	150.08	189.99	5.01	9.90	7.00
				Estimated $C_{in}(t)$ for Case 3					
3	1.00	0.30	0.50	130.01	149.98	190.00	4.99	10.02	6.99
				Estimated $C_{in}(t)$ for Case 4					
3	0.99	0.30	0.50	130.25	151.03	189.94	5.29	9.18	7.13
				Estimated $C_{in}(t)$ for Case 5					
3	0.98	0.29	0.51	130.13	150.55	190.05	5.25	9.67	6.95
				Estimated $C_{in}(t)$ for Case 6					
3	1.01	0.32	0.53	129.58	148.54	189.59	4.35	11.28	6.43
				Estimated $C_{in}(t)$ for Case 7					
3	7.26	0.41	0.39	128.33	142.32	192.37	0.58	12.66	8.88

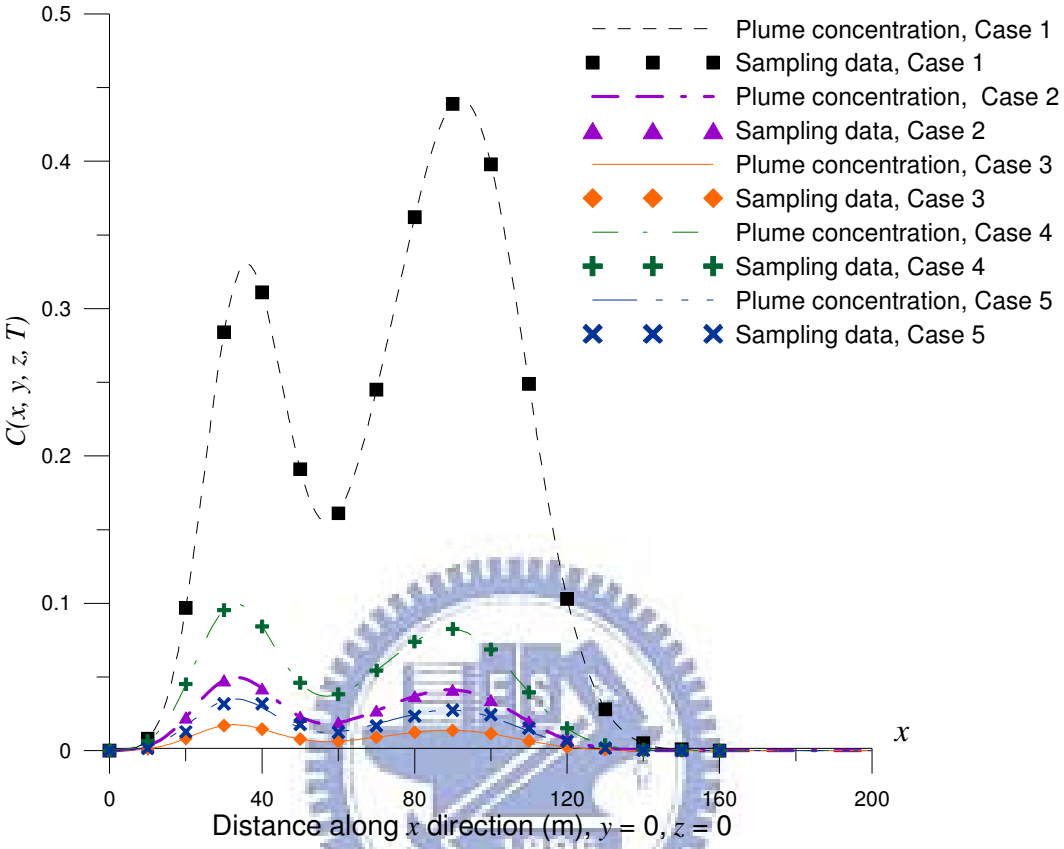

Fig. 1. Scenario 1: sampling data at 225 days.

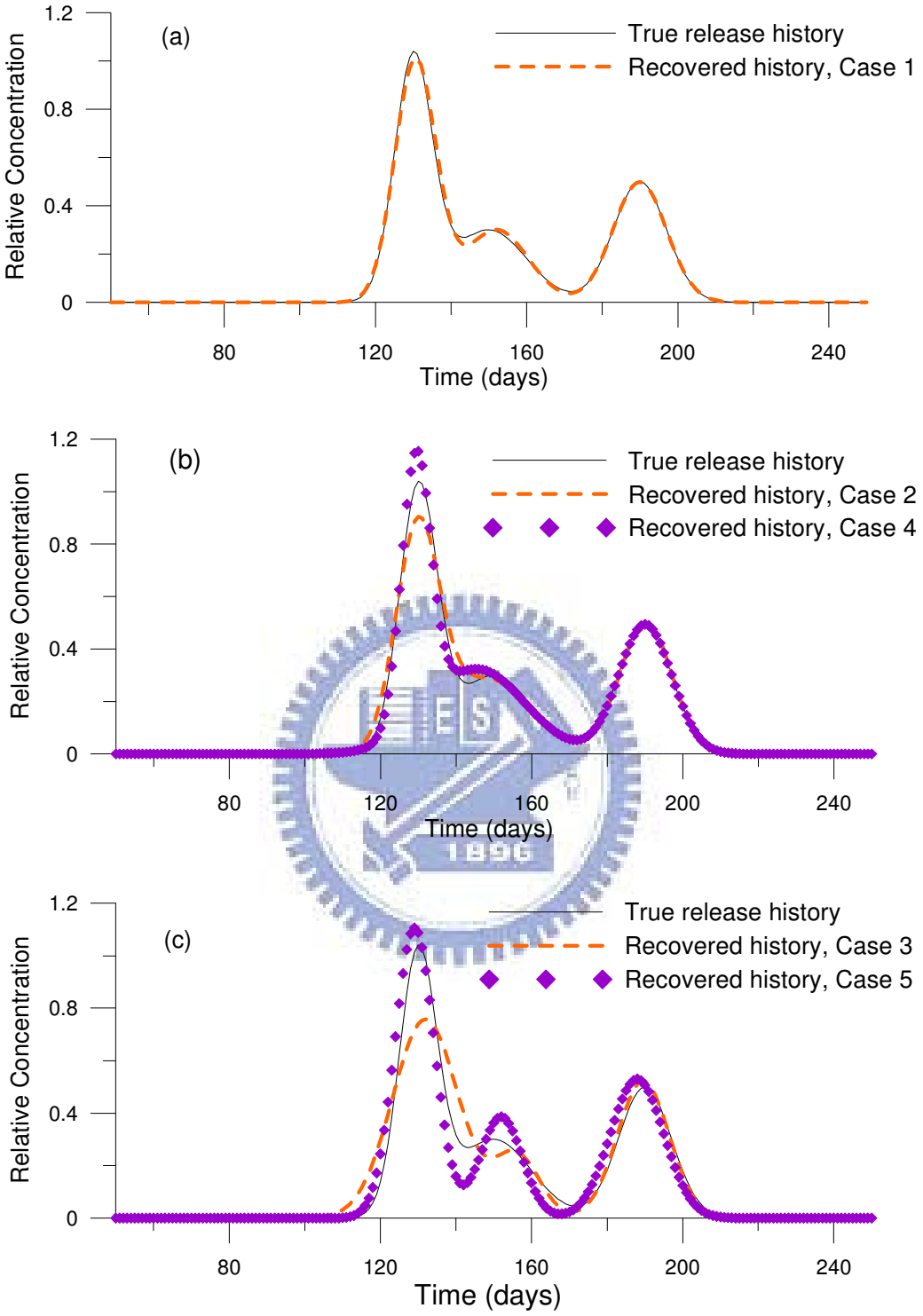

Fig. 2. Scenario 1: the recovered source release histories for cases 1 – 5.

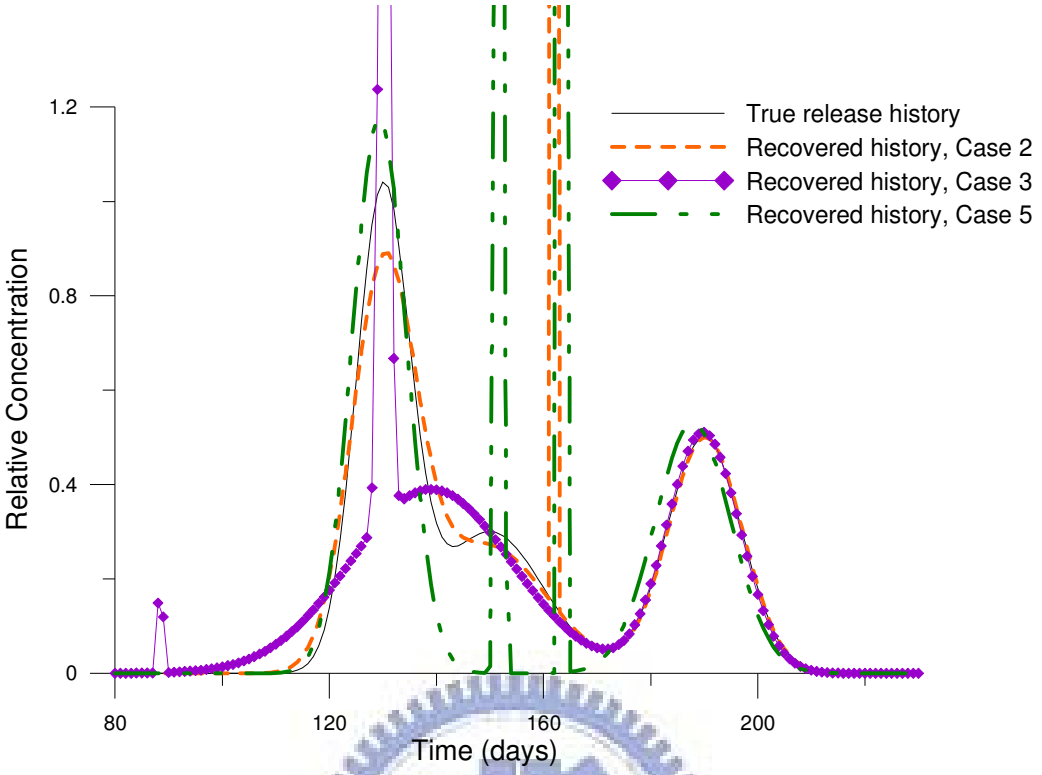

Fig. 3. Scenario 1: the recovered source release history when $k = 4$ for cases 2, 3, and 5.

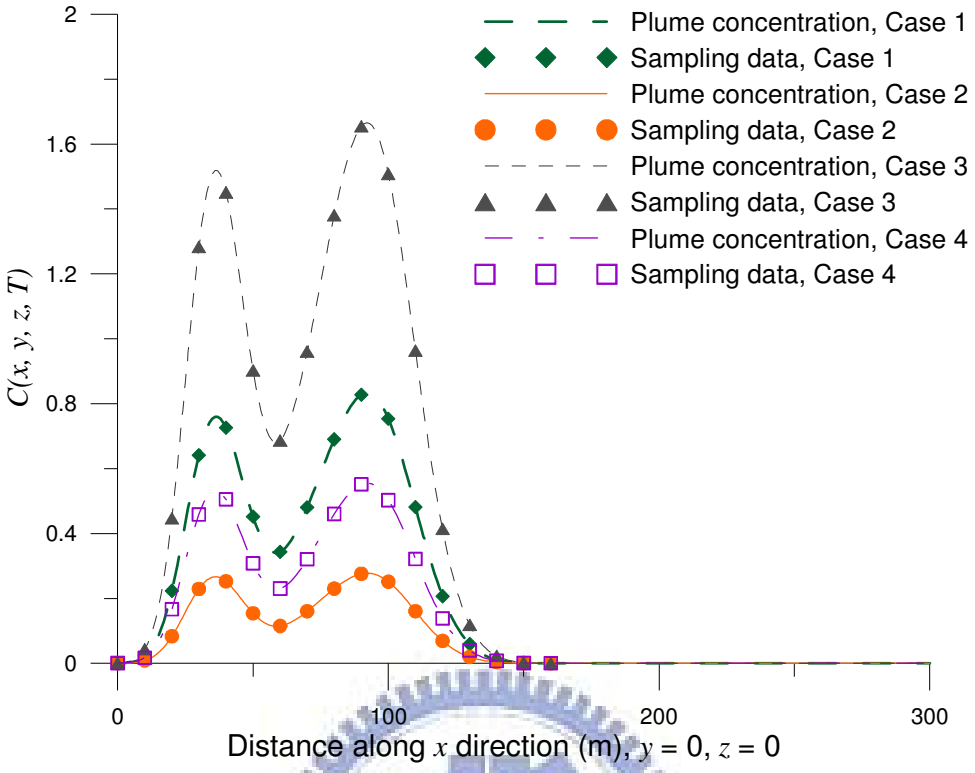

Fig. 4. Scenario 2: Sampling data at 225 days.

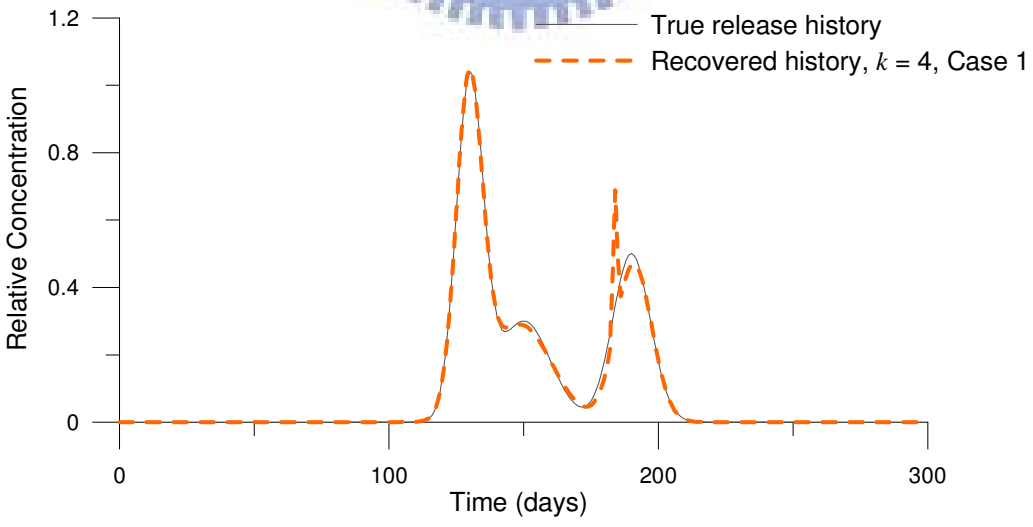

Fig. 5. Scenario 2: the recovered source release history when $k = 4$ for case 1.

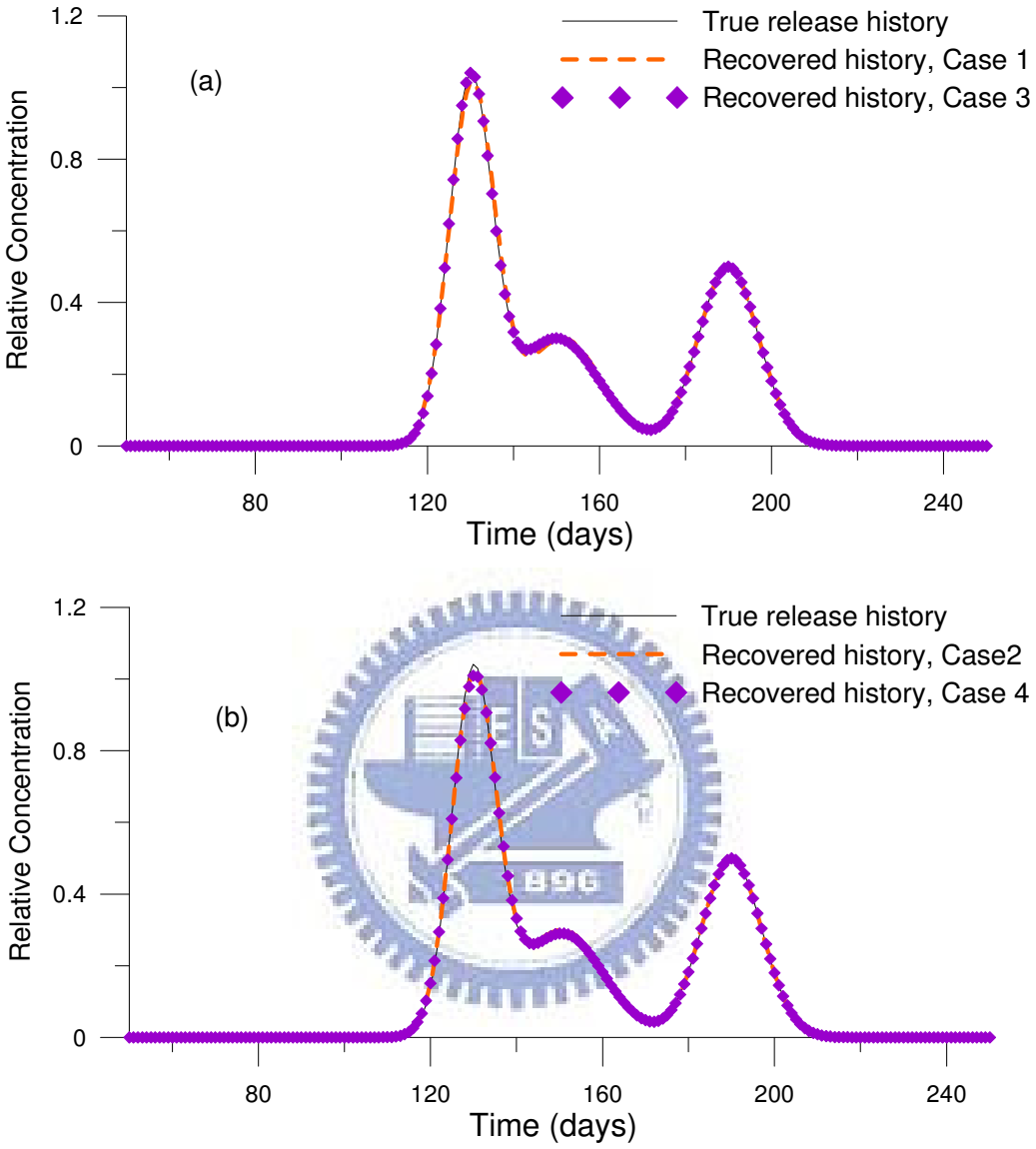

Fig. 6. Scenario 2: the recovered source release histories for cases 1 – 4.

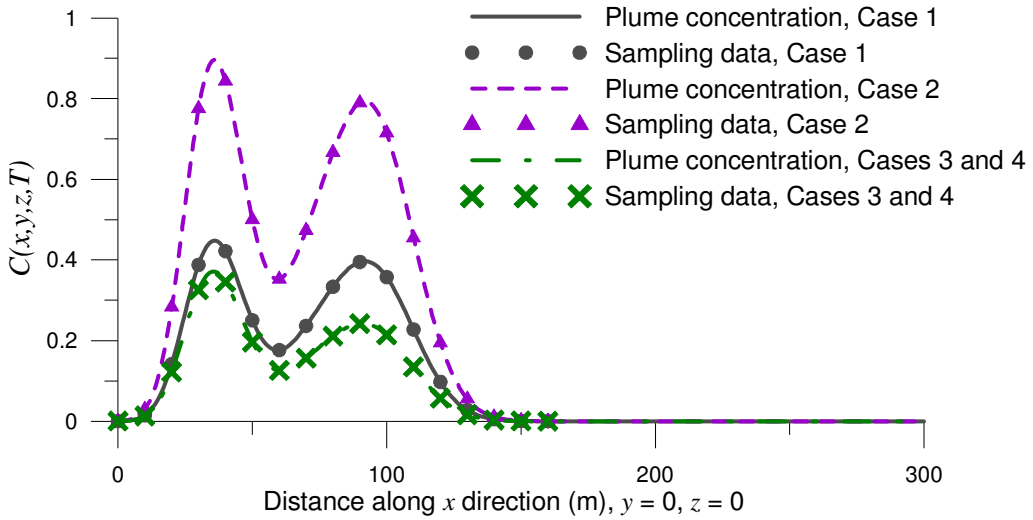

Fig. 7. Scenario 3: sampling concentration at 225 days.

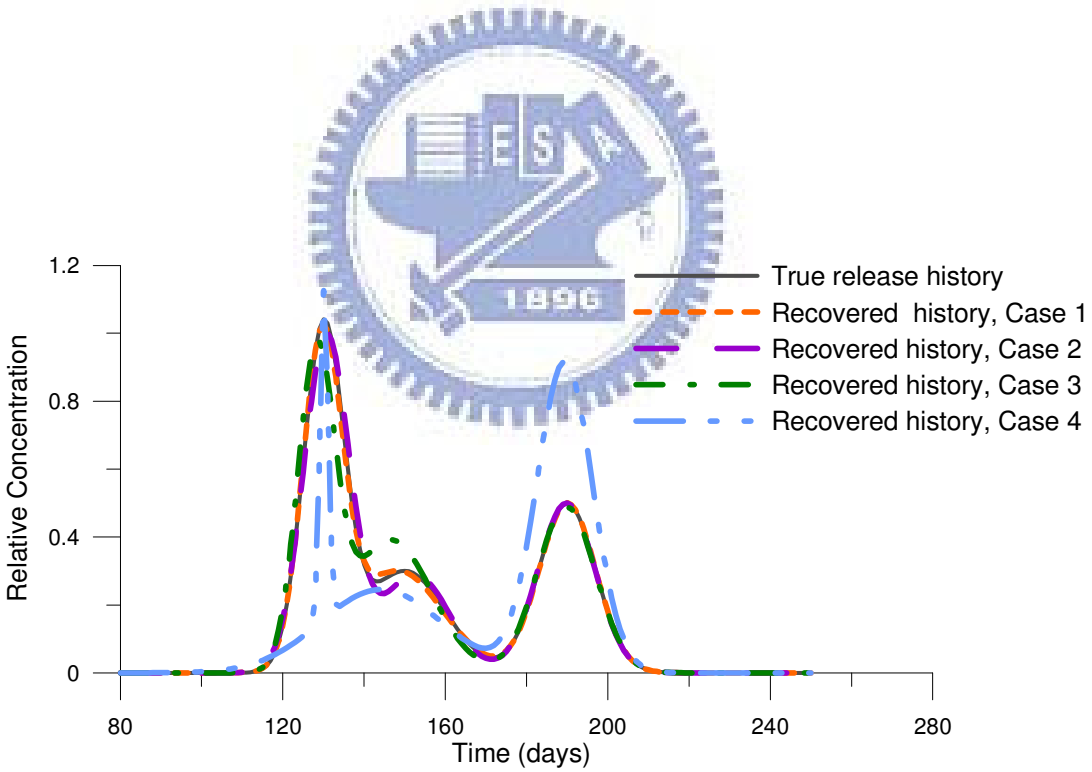

Fig. 8. Scenario 3: the recovered source release histories for cases 1 – 4.

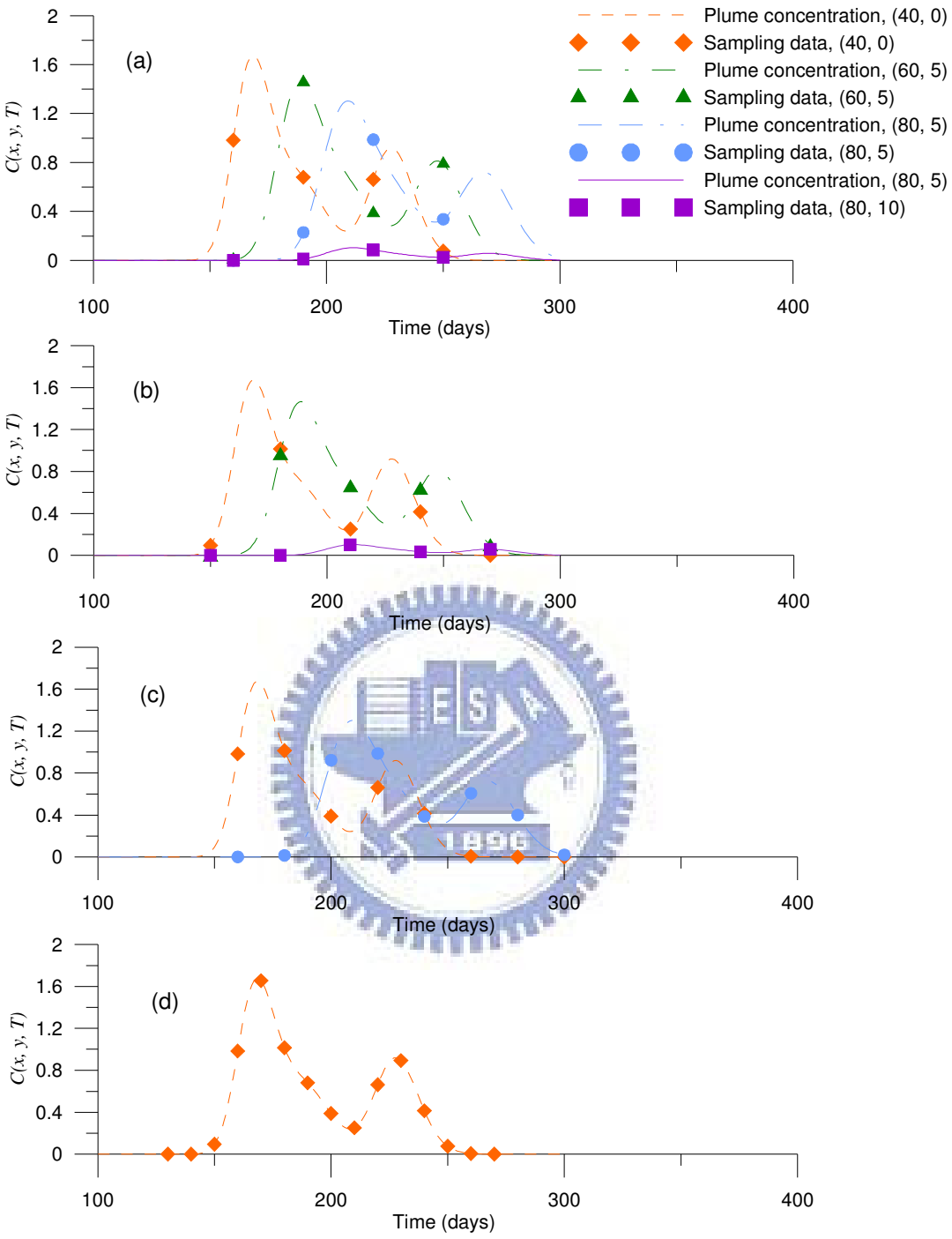

Fig. 9. Scenario 4: (a) case 1, 4 wells with 16data; (b) case 2, 3 wells with 15data; (c) case 3, 2 wells with 16data; and (d) case 4, 1well with 15data.

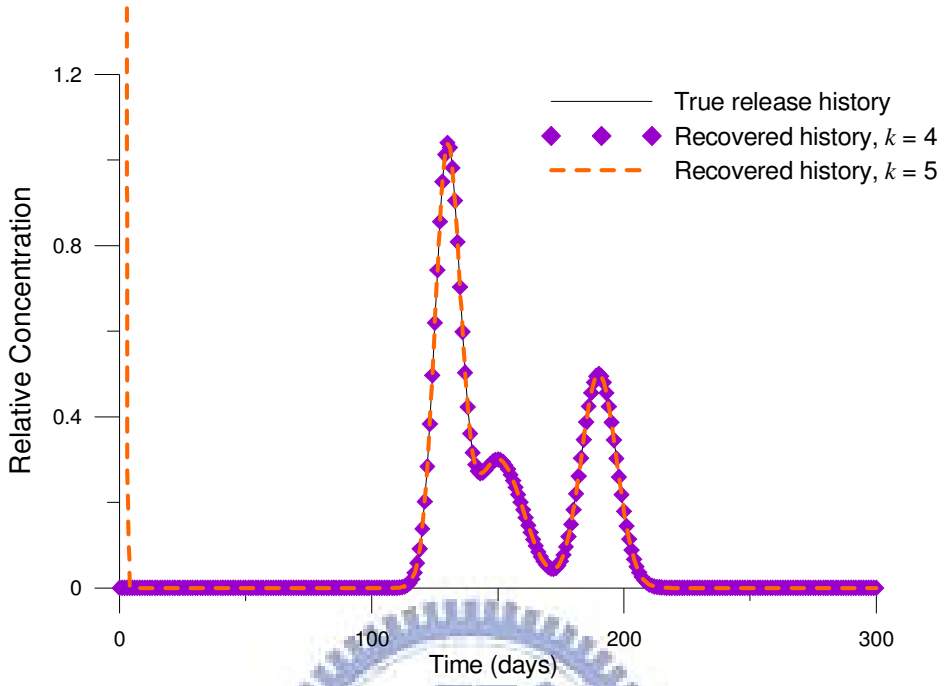

Fig. 10. Scenario 4: the recovered source release history when k = 4 and 5 for case 1.

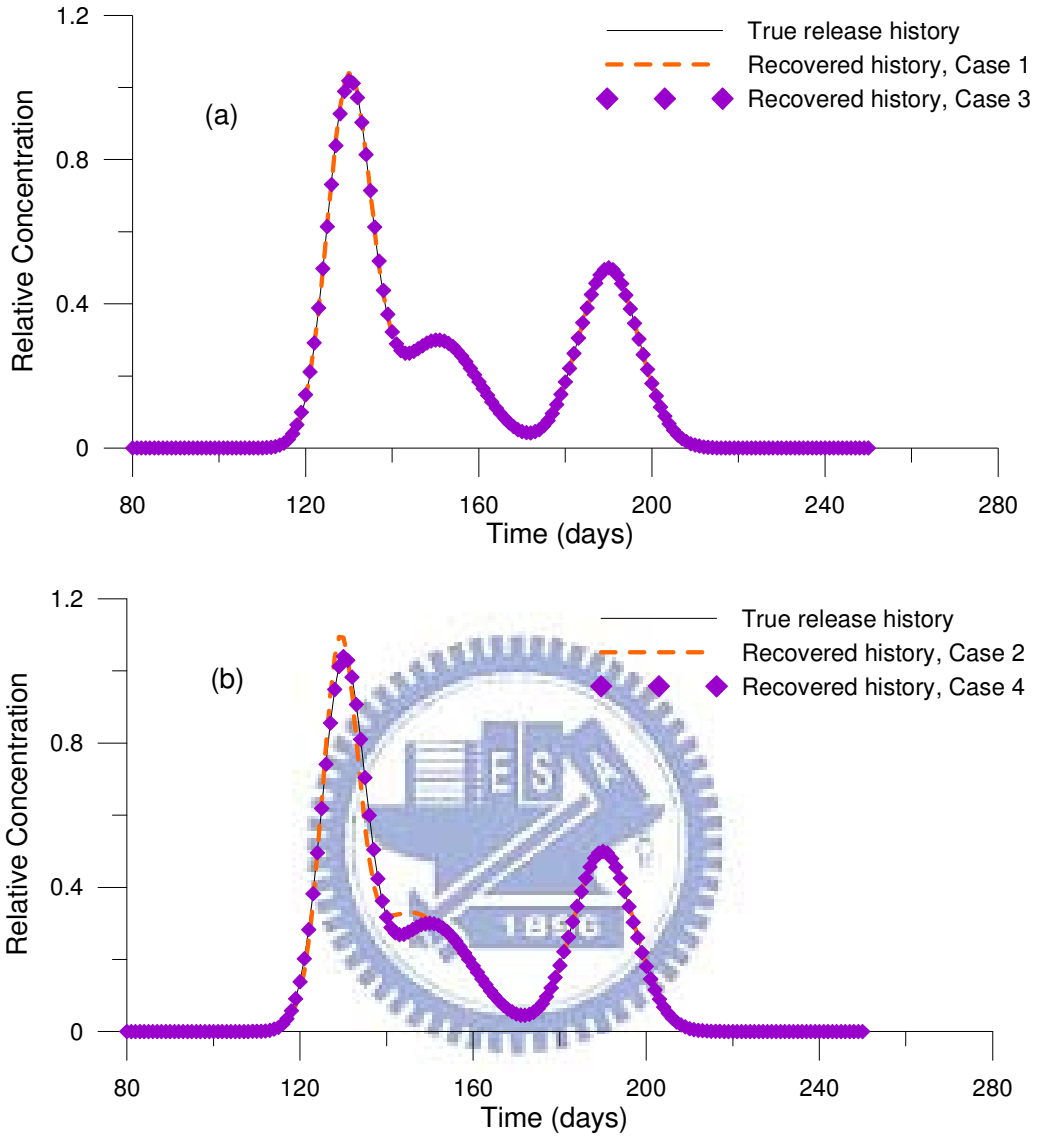

Fig. 11. Scenario 4: the recovered source release histories for cases 1 – 4.

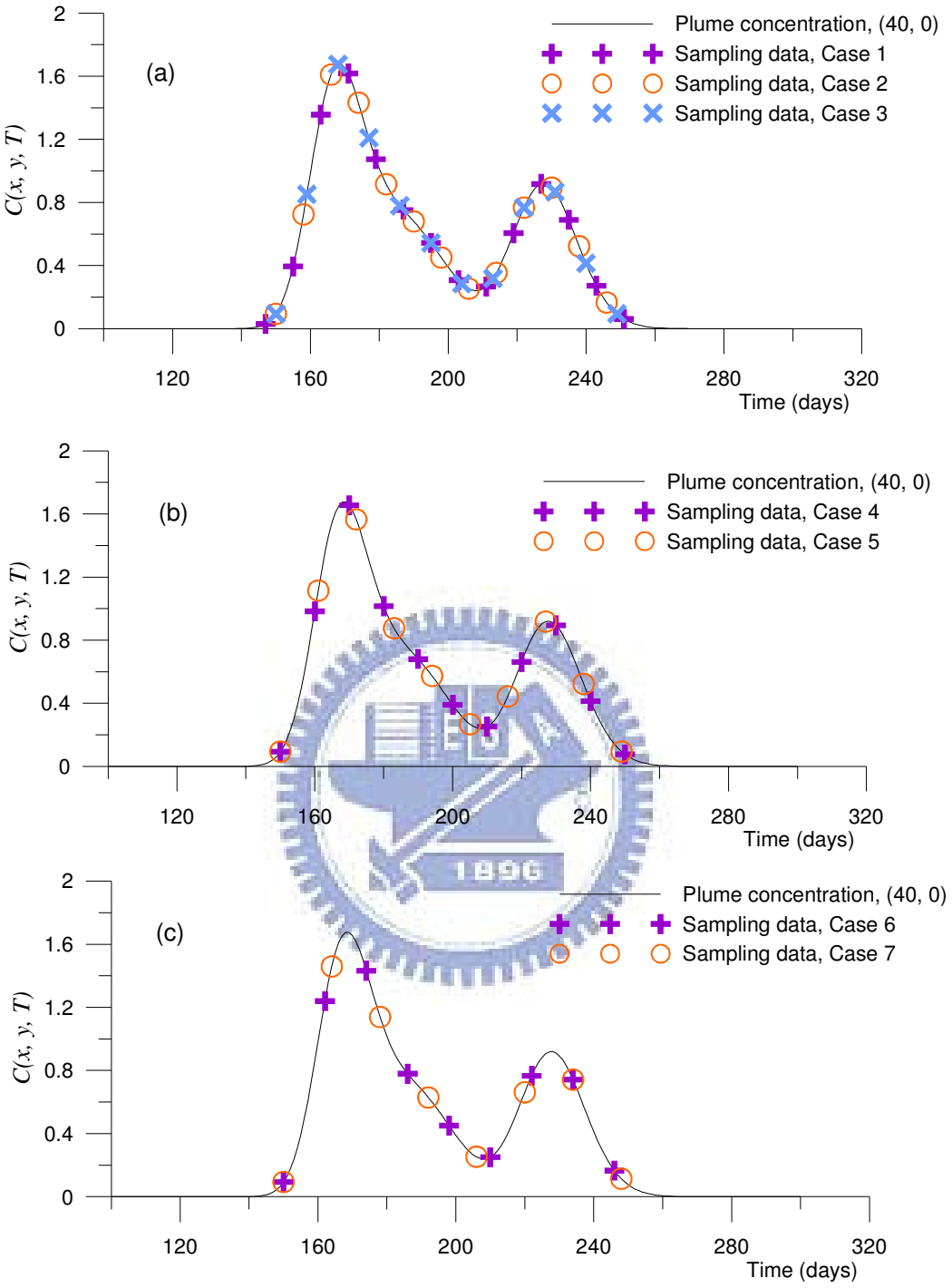

Fig. 12. Scenario 5: different number of sampling data at (40, 0) for cases 1 – 7.

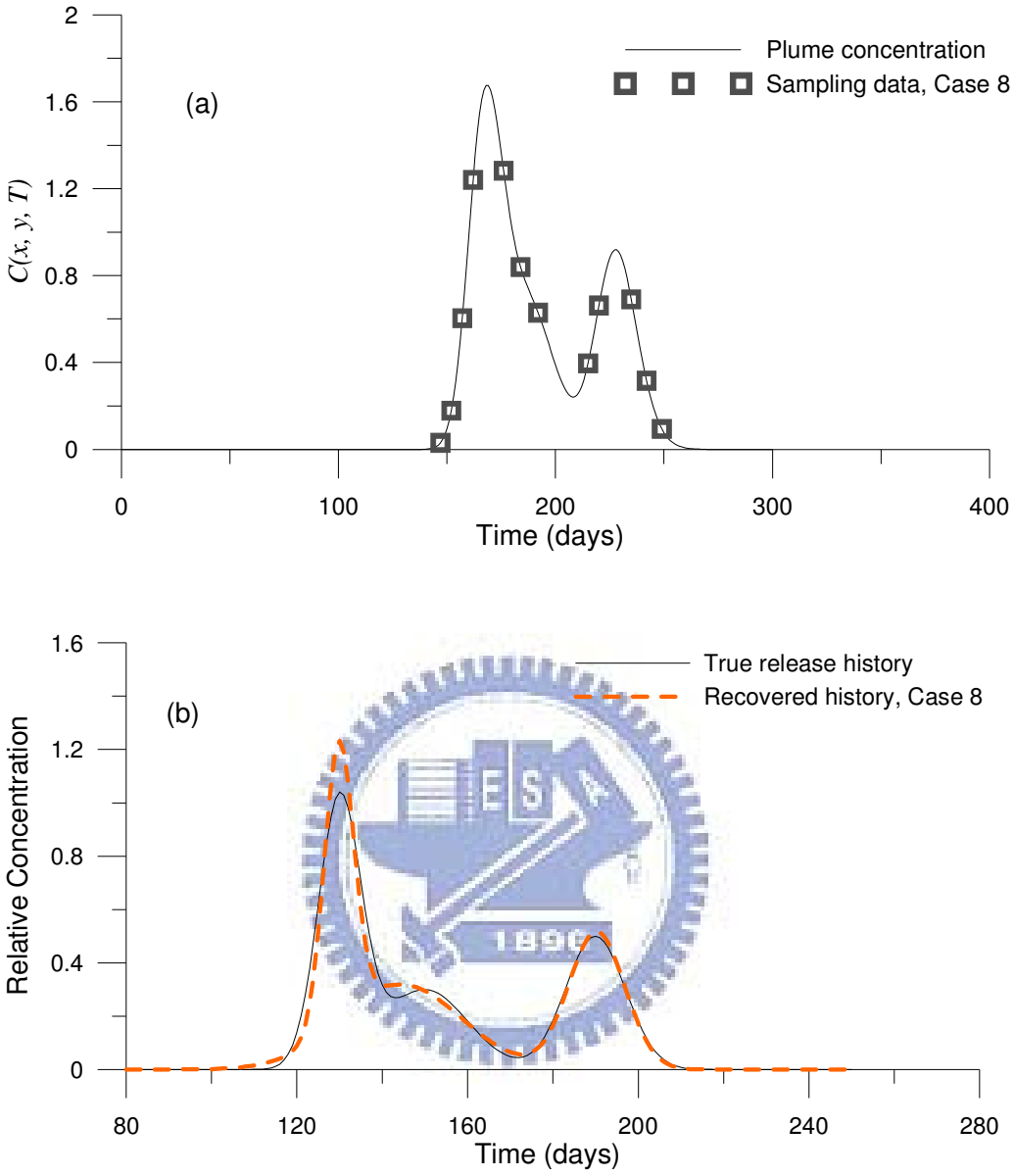

Fig. 13. Case 8 in scenario 6: (a) data sampled at (40, 0) from 147 to 249 days; (b) the recovered source release history.

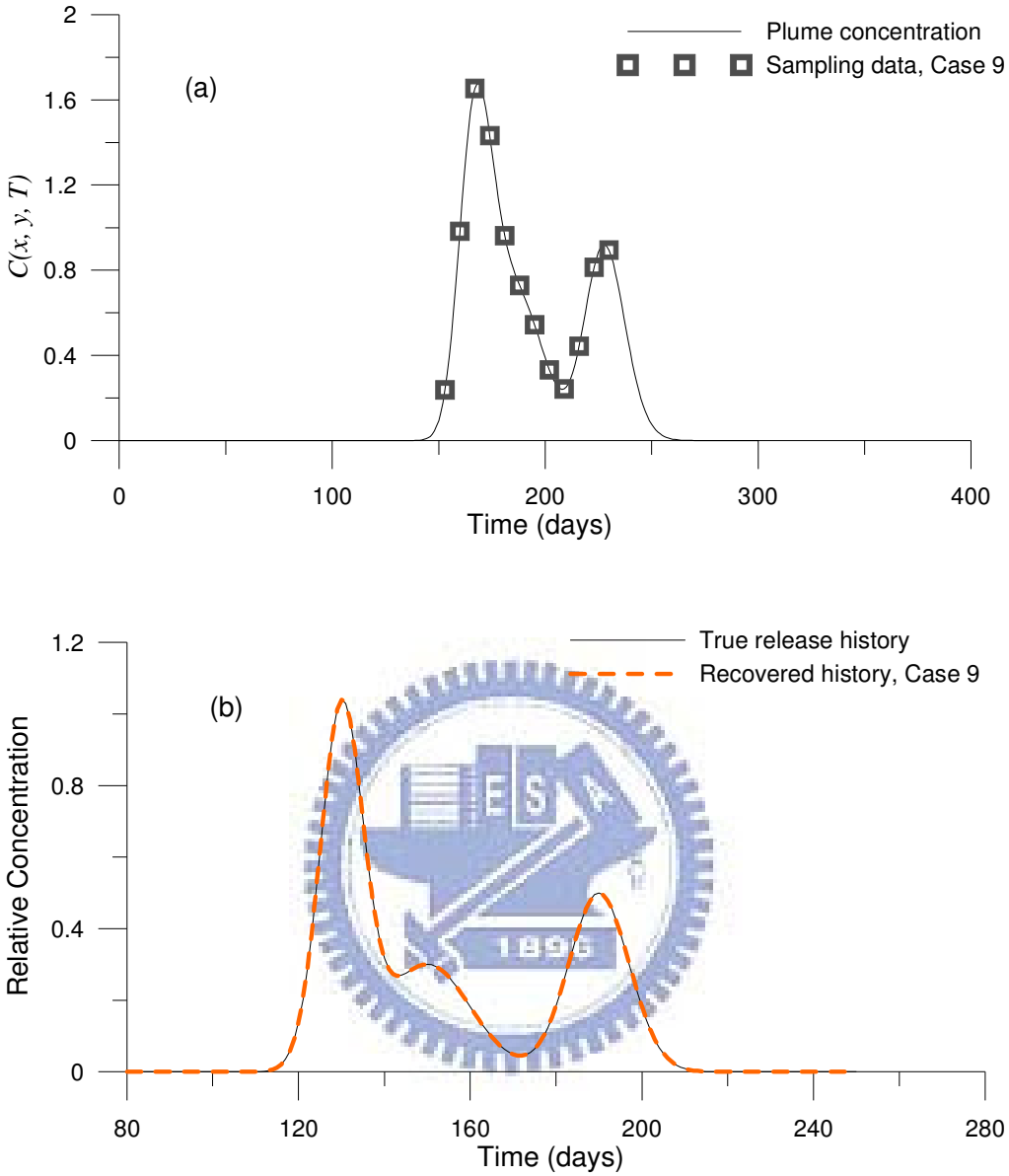

Fig. 14. Case 9 in scenario 6: (a) data sampled at (40, 0) from 153 to 230 days; (b) the recovered source release history.

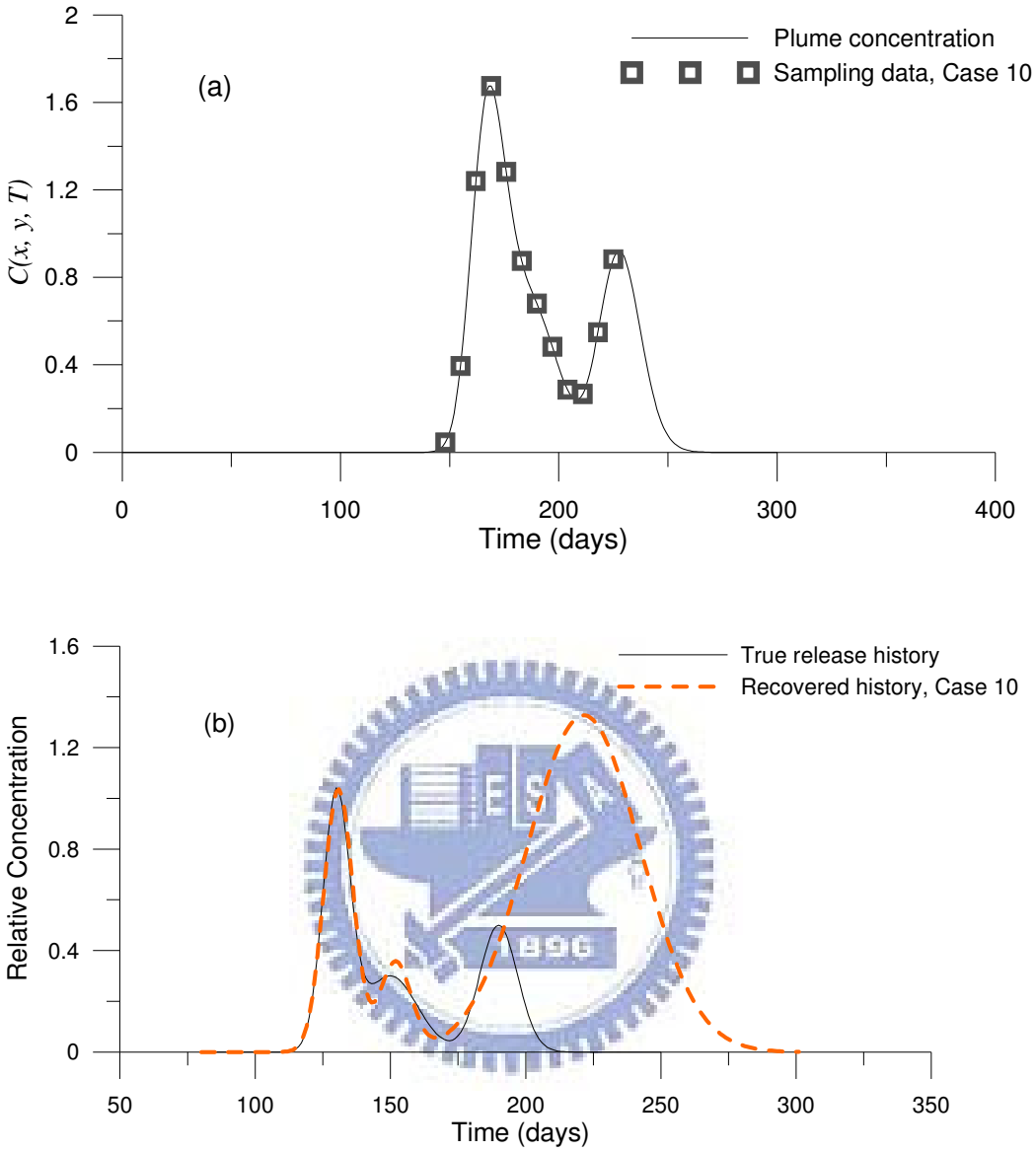

Fig. 15. Case 10 in scenario 6: (a) data sampled at (40, 0) from 148 to 225 days; (b) the recovered source release history.

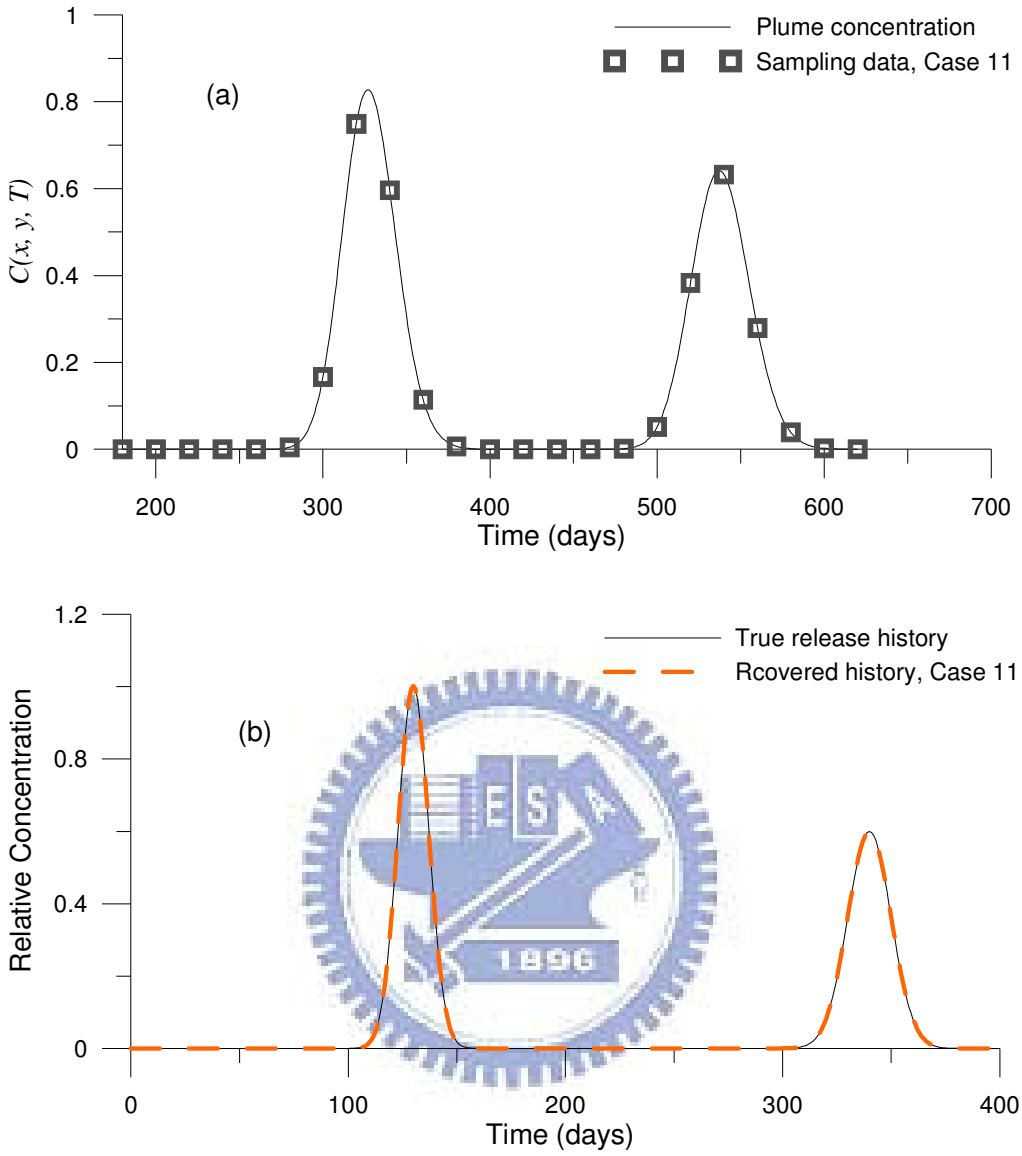

Fig. 16. Case 11 in scenario 6: (a) data sampled at (200, 0) from 180 to 620 days; (b) the recovered source release history.

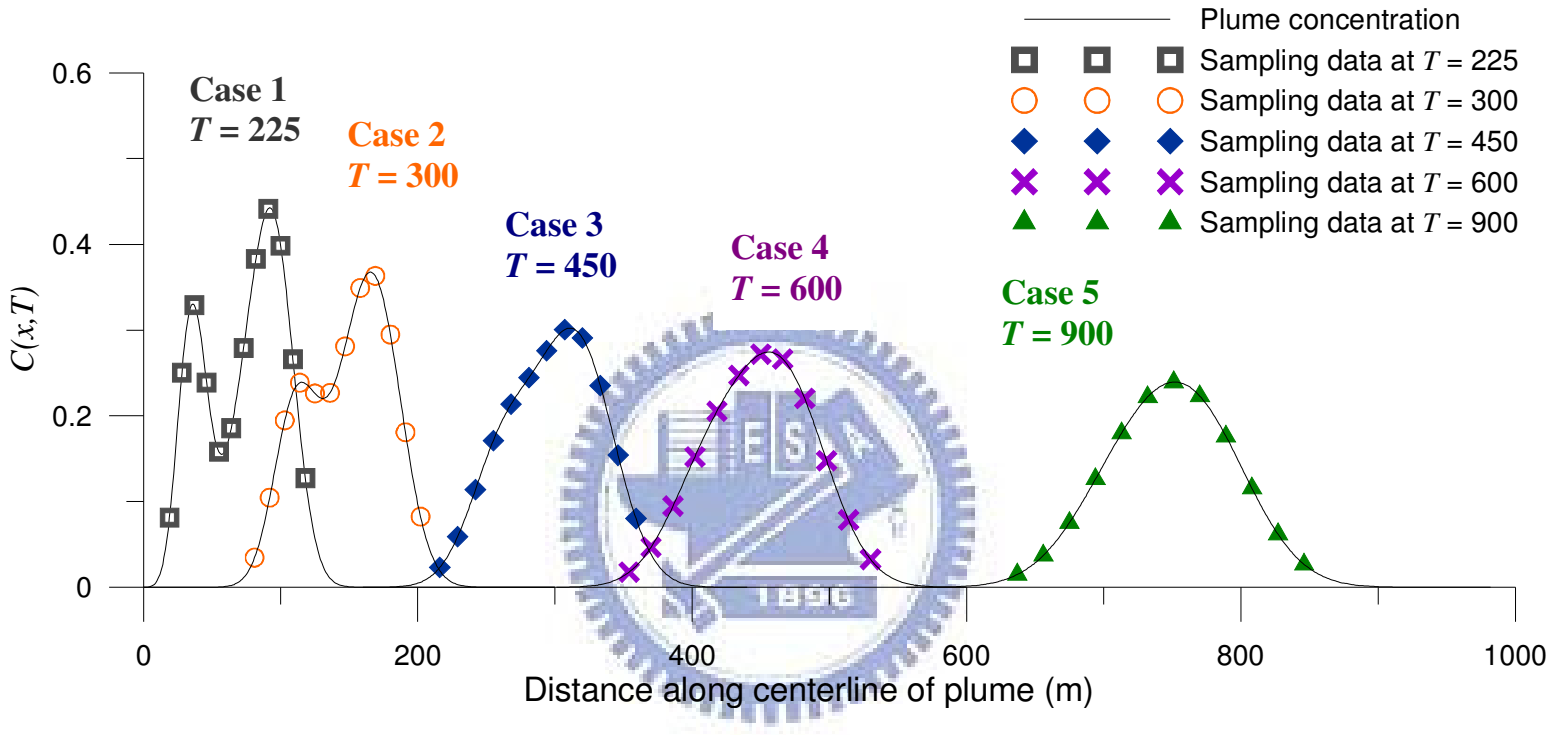

Fig. 17. Scenario 7: nine sampling data sampled within the region of 95 % of contaminant mass.

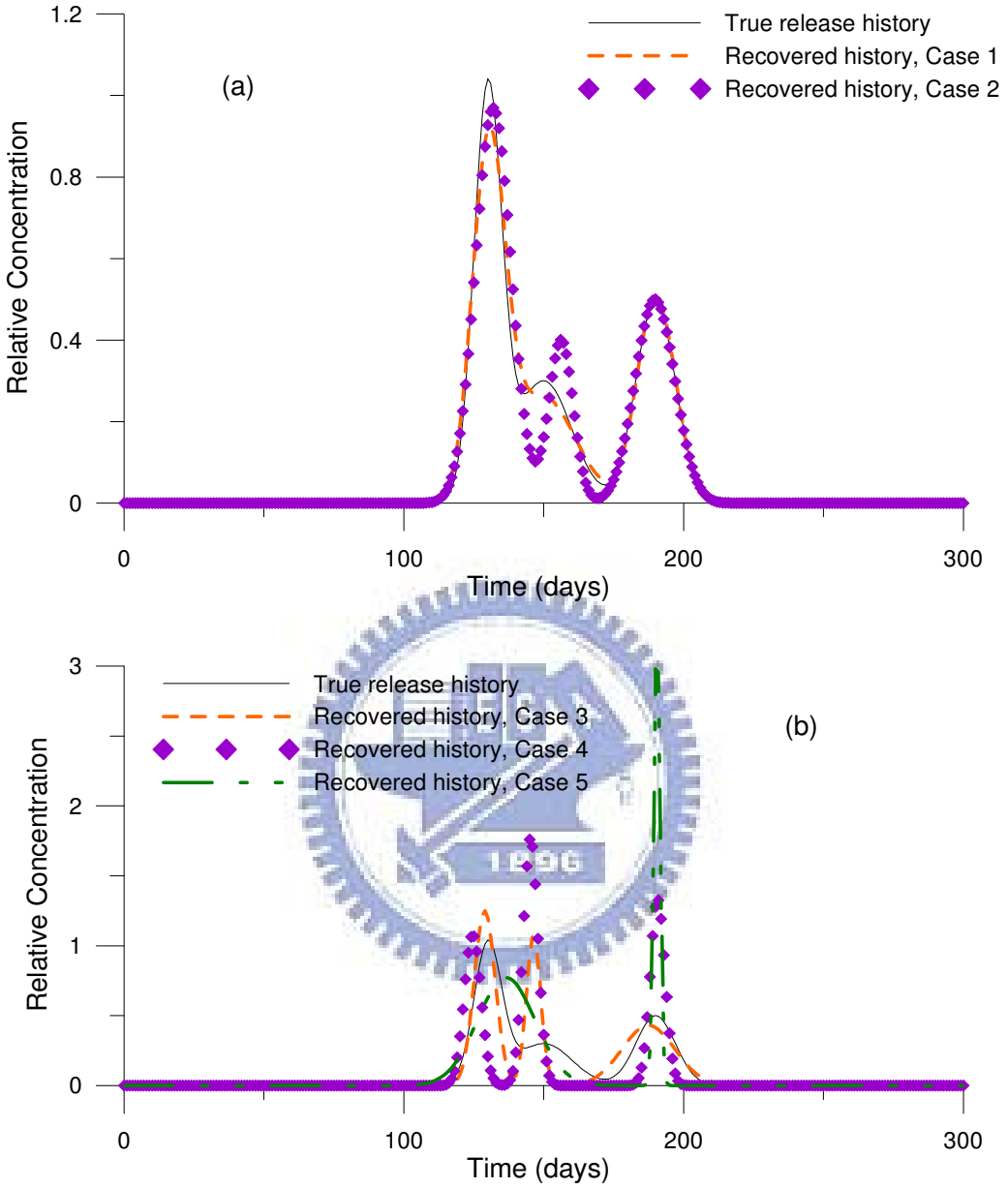

Fig. 18. Scenario 7: the recovered source release histories for cases 1 – 5.

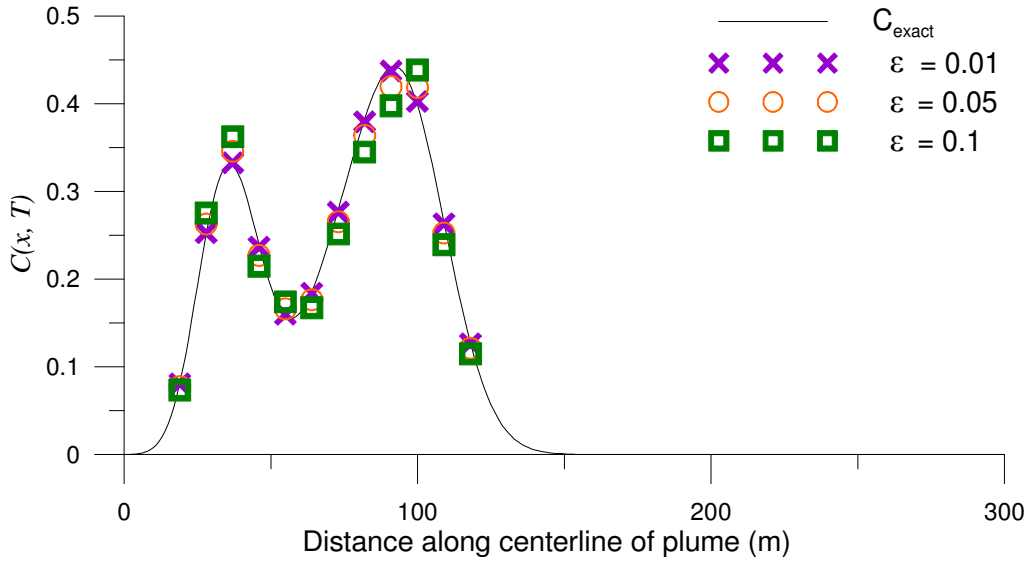

Fig. 19. Scenario 8: erroneously sampling data at $T = 225$ days. Case 1, $\varepsilon = 0.01$; case 2, $\varepsilon = 0.05$; case 3, $\varepsilon = 0.1$.

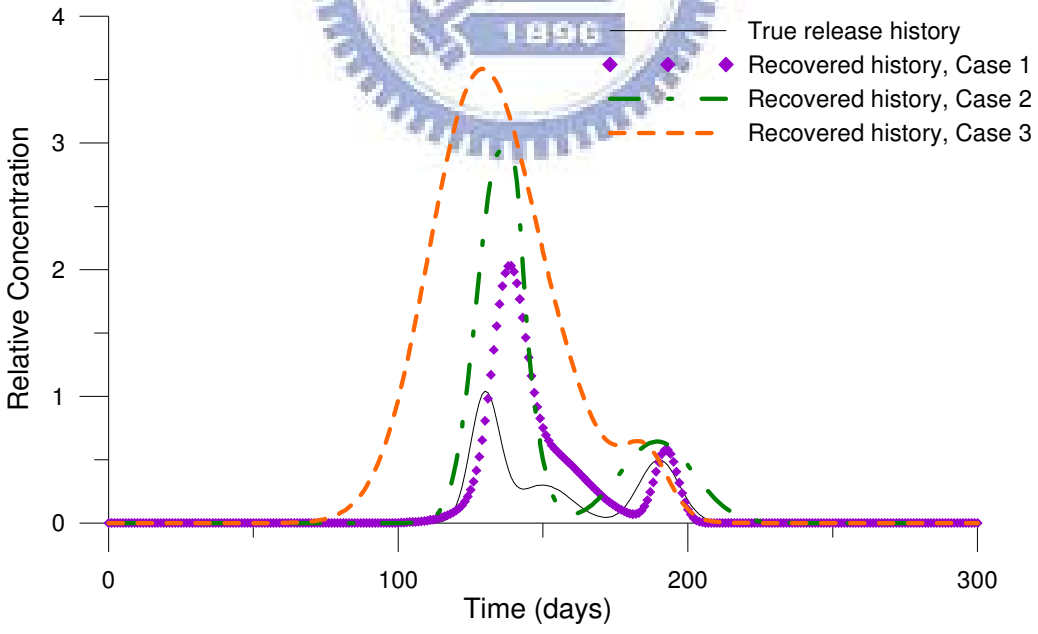

Fig. 20. Scenario 8: the recovered source release histories for cases 1 – 3.

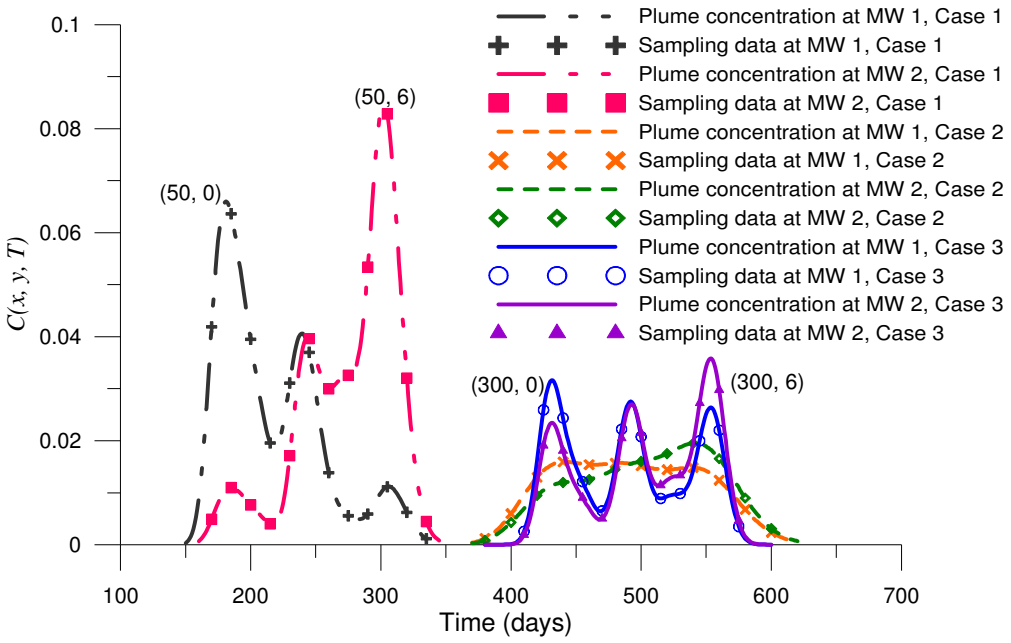

Fig. 21. Scenario 9: the sampling data at MWs 1 and 2 for cases 1 – 3.

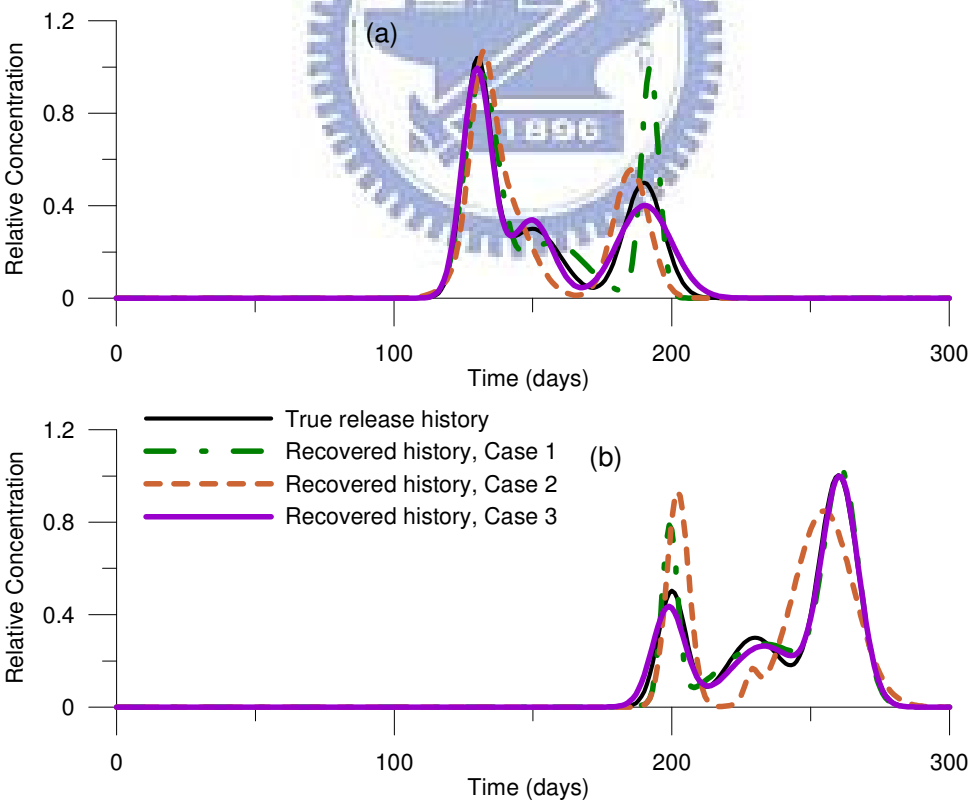

Fig. 22. Scenario 9: the recovered release histories of (a) source 1 and (b) source 2, for cases 1 – 3.

個人資料

姓名：陳淇汾

生日：民國 70 年 6 月 16 日

出生地：台北縣

電話：02-26013112

住址：台北縣林口鄉中正路 74 巷 5 弄 2 號

學歷：民國 92 年畢業於私立淡江大學水資源與環境工程學系

民國 95 年畢業於國立交通大學環境工程研究所